

Northumbria Research Link

Citation: Bilal, Muhammad, Sultan, Muhammad, Morosuk, Tatiana, Den, Walter, Sajjad, Uzair, Aslam, Mian MA, Shahzad, Muhammad Wakil and Farooq, Muhammad (2022) Adsorption-based atmospheric water harvesting: A review of adsorbents and systems. International Communications in Heat and Mass Transfer, 133. p. 105961. ISSN 0735-1933

Published by: Elsevier

URL: <https://doi.org/10.1016/j.icheatmasstransfer.2022....>
<<https://doi.org/10.1016/j.icheatmasstransfer.2022.10596>>

This version was downloaded from Northumbria Research Link:
<https://nrl.northumbria.ac.uk/id/eprint/48680/>

Northumbria University has developed Northumbria Research Link (NRL) to enable users to access the University's research output. Copyright © and moral rights for items on NRL are retained by the individual author(s) and/or other copyright owners. Single copies of full items can be reproduced, displayed or performed, and given to third parties in any format or medium for personal research or study, educational, or not-for-profit purposes without prior permission or charge, provided the authors, title and full bibliographic details are given, as well as a hyperlink and/or URL to the original metadata page. The content must not be changed in any way. Full items must not be sold commercially in any format or medium without formal permission of the copyright holder. The full policy is available online: <http://nrl.northumbria.ac.uk/policies.html>

This document may differ from the final, published version of the research and has been made available online in accordance with publisher policies. To read and/or cite from the published version of the research, please visit the publisher's website (a subscription may be required.)

Adsorption-based atmospheric water harvesting: A review of adsorbents and systems

Muhammad Bilal ^{a,†}, Muhammad Sultan ^{a,†,*}, Tatiana Morosuk ^b, Walter Den ^c, Uzair Sajjad ^d, Mian MA Aslam ^e, Muhammad W. Shahzad ^f, Muhammad Farooq ^g

^a Department of Agricultural Engineering, Bahauddin Zakariya University, Bosan Road, Multan 60800, Pakistan

^b Institute for Energy Engineering, Technische Universität Berlin, Marchstr. 18, 10587, Berlin, Germany

^c Department of Mathematical, Physical, and Engineering Sciences, Texas A&M University-San Antonio, One University Way, San Antonio, Texas 78224, USA

^d Department of Energy and Refrigerating Air-Conditioning Engineering, National Taipei University of Technology, Taipei 10608, Taiwan

^e Department of Environmental Science and Engineering, Tunghai University, No. 1727, Section 4, Taiwan Boulevard, Xitun District, Taichung City, 407, Taiwan

^f Department of Mechanical and Construction Engineering, Northumbria University, Newcastle Upon Tyne, NE1 8ST, United Kingdom

^g Department of Mechanical Engineering, University of Engineering and Technology, 39161 Lahore, Pakistan

[†] These authors contributed equally to this work.

*Corresponding Authors Email: muhammadsultan@bzu.edu.pk ; Tel: +92-333-610-8888

Abstract

Atmospheric water harvesting (AWH) has been an appealing prospect for decades to overcome water scarcity in remote areas. Adsorption-based AWH technologies have gained popularity due to their adaptability, and applicability using low-grade heat sources. This study presents up-to-date and future possibilities of adsorbents and systems for adsorption-based AWH. In this review, in-depth advancements in adsorbent materials are compartmentalized into adsorption equilibrium/isotherms, adsorption kinetics, and thermal conductivity. Various systems designs and modifications have been reviewed and classified accordingly. Liquid desiccants i.e., CaCl₂ and LiCl-based AWH systems produced in between 0.63 to 1.0 kg/m/d of water. Recently, metal-organic frameworks (MOFs) are realized as effective adsorbents for AWH. Their excellent hydrophilicity, structural integrity, and tailorable structures can provide water in high and low relative humidity (RH) areas. MOF-841 and MOF-801 yielded maximum adsorption uptakes at 25 °C i.e., 0.5 and 0.3 g/g, respectively. MOF-801 showed an excellent water production of 0.2-0.3 L/kg/d at 5%-40% RH and 20-40°C. MOF-303 delivered ~0.7 L/kg/d at 10% RH and 27°C. Cr-soc-MOF-1 and MIL-101(Cr) resulted in maximum adsorption uptakes i.e., 1.9 g/g and 1.4 g/g, respectively. Future possibilities regarding these captivating and emerging adsorption technologies are discussed as concluding remarks.

Keywords: atmospheric water harvesting; adsorbents; technologies; systems; metal-organic framework; solid and liquid desiccants

1 Introduction

Water shortage is among the unavoidable worldwide challenges identified by the United Nation and the degree of water stress is expected to worsen in the foreseeable future [1]. About 90% of the global

population resides in developing countries, thus exerting more pressure on water resources due to high population densities and growth rates [2]. In a recent study, more than 65% population of the world will live in a water-scarce condition by 2025 because of the growing population density and the lack of modern water supply infrastructure [3,4]. Moreover, the uneven distribution of freshwater, particularly in geographic regions historically having sparse rainfalls, face significant public health hazards due to lack of access to water [5]. Freshwater only constitutes a small portion (i.e., ~2.5%) and saltwater in oceans accounts for the rest (i.e., ~97.5%) of the total global water. However, only 0.4% of the freshwater sources are readily available in the forms of lakes, soil moisture, atmospheric water vapors, wetlands, rivers, and biota i.e., 67.4%, 12.2%, 9.5%, 8.5%, 1.6%, and 0.8%, respectively [6]. The limited freshwater resources put more than half of the global population (about 4 billion people) in peril of constant water shortage [7,8]. According to a United Nations report, 31 countries are at the physical water stress threshold value (i.e., 25 to 70%), and 22 countries are above the physical water stress threshold value (i.e., >70%) [9]. South and Central Asia, North Africa, and the Middle East will be under severe water stress by 2050 [10]. Due to the continuous degradation of freshwater resources and the increasing threat of climate change, developing viable options for freshwater generation for the water-stressed countries is an urgent matter. Desalination of oceanic water has been proven a viable option for the provision of fresh potable water but it is only feasible for coastal regions [11–13]. Conversely, in landlocked regions, especially those in arid and semi-arid climate conditions, AWH could prove as a key to overcoming the water shortage challenge because it provides safe potable water at a small communal level without affecting the environment [14]. AWH techniques have been administered dating back to the early 1900s by Edger S. Belden (US661944A). Nowadays, fresh potable water could be provided using AWH (i.e., ~13000 trillion liters readily available for extraction) [6]. The atmosphere contains around ~10% of all freshwater in the form of molecules [15,16]. Commonly, two methods have been used for the AWH, namely sub-dewpoint cooling, and adsorption of atmospheric water using desiccants. Fig. 1 compartmentalizes the three mainstream techniques to capture, collect, and harvest atmospheric water, including (i) active cooling where water is extracted with an external energy source, e.g., vapor compression, Peltier cooling, and membrane-assisted harvesting; (ii) passive cooling where water is harvested without an external energy system, e.g., dew collection, and fog harvesting; (iii) desiccation where air moisture is adsorbed and absorbed through a sorbent material. In general, a successful AWH technology must fulfill the criteria of cost effective, energy efficient, safe, chemically stable, and independent of high-grade energy sources. In the context of thermodynamics, the main design consideration is the energy efficiency of the process [17].

Fig. 1 is inserted here.

The authors aim to review the different AWH technologies, their current applications, prospects, and challenges. By comparison, adsorption-based AWH technology offers a relatively cost-effective, environment-friendly, decentralized technique that operates with low-grade thermal energy. To date, adsorption-based AWH has gained renewed interest by researchers and practitioners due to its adaptability and mobility [18–21]. Primarily, this review presents the most updated view regarding the adsorption-based AWH technologies on both system design and the adsorbent materials. Furthermore, the present study compiles a comprehensive review on the in-depth advancements in adsorbent materials and categorized them into

adsorption equilibrium/isotherms, adsorption kinetics, and thermal conductivity. So far, many AWH adsorbent materials and systems have been developed. Capable of sub-dewpoint temperature cooling, an apparatus was presented in 1963 which consisted of an inclined and a vertical channel [22]. Three years later, a solar still was introduced, in which ethylene glycol was used as a liquid desiccant for AWH [23]. Almost a decade and a half later, in 1981, a solid desiccant material was used instead of liquid desiccants for AWH [24]. Nearly, half a decade later, in 1987, “s” shaped composite desiccant material instead of liquid and conventional solid desiccants was developed for AWH [25]. In 1998, innovative desiccant materials were developed in Russia for AWH, capable of collecting 3 to 5 tons of water [26]. Fig. 2 shows some of the published patents in the field of AWH. To illustrate the growing interest in AWH, the number of research publications depicted in Fig. 3 further reflects the fast-expanding rate of technological development in recent years.

Fig. 2 is inserted here.

Fig. 3 is inserted here.

2 Active and passive AWH technologies

2.1 Vapor compression cycle based AWH

Harvesting condensates is a common practice in large-scale air conditioning applications [27,28]. Dehumidifiers based on an active air-cooling process mostly consist of a conventional vapor compression cycle (VCC) of liquid refrigerants to transfer heat between the evaporator (a cold reservoir) and the condenser (a hot reservoir). Fig. 4 presents the VCC-based AWH process. Similarly, a VCC-based AWH device was developed for military purposes [29]. The reported water harvesting rate (WHR) for this device was 1.50 kg h⁻¹. Simulation of a small-scale VCC prototype showed a WHR of range 0.92-1.08 kg h⁻¹ under 24 hours operational time [30]. A VCC system was installed in Iraq under conditions in which the airflow rate across the evaporator was studied. The maximum water production for this system was 7.9 L per day at an air flow of 230 m³ h⁻¹ [31]. Refrigerants used in these devices predominately were 1,1,1,2-tetrafluoroethane, ammonia, isobutane and chlorofluorocarbons (CFCs) [32–34]. These refrigerants are known as ozone-depleting chemicals and have been replaced with more environment-friendly and cost-effective refrigerants, i.e., R143a [35].

Fig. 4 is inserted here.

2.2 Thermoelectric cooling based AWH

In addition to VCC, the Peltier effect – also known as thermoelectric cooling (TEC) – is another common approach to reach the dew point temperature [36]. These TEC devices are compact and powered by direct current. Zhang et al. (2010) performed a feasibility study in remote areas using TEC powered device in which the optimum temperature of the semi-conductor material for AWH ranges from -130°C to 90°C [37]. An experimental and simulation study was conducted on TEC processes for water extraction using a material coded as TEC1-12706, resulting in a WHR per chip of 0.007 kg h⁻¹ at a volumetric air flow of 4.8 m³ h⁻¹ [38]. A TEC based water condensation system powered by solar cells was reported which produced up to 1 L h⁻¹

[39]. Another study reported water generation through TEC principle, shown in Fig. 5, capable of harvesting 26 ml h⁻¹ of water at 75% RH [40]. Table 1 shows the features of VCC and TEC systems with 7500 L d⁻¹ and 1500 L d⁻¹ water production capacities. These VCC-based devices can be designed to reach dew points less than 4.5°C but are energy-intensive [41].

Fig. 5 is inserted here.

Table. 1 is inserted here.

2.3 Membrane-based AWH

Membranes can be used for AWH using active cooling. The efficiency of such methods is mainly influenced by physical parameters of the membrane i.e., water permeability. Bergmair et al. (2014) performed an analysis for membrane-based AWH to selectively separate water vapors from the air. These vapors are then condensed into liquid form. Through system optimization, such membrane-based systems can result in a WHR of ~9 m³ d⁻¹ as compared to those that produce ~4.5 m³ d⁻¹ without membrane modules. Membrane modules in atmospheric water generation reduce energy costs by more than 50% [42]. The same research group further studied the effect of different driving forces across the membrane module on AWH via a combination of vacuum pump and recirculation of sweep air at low pressure [43]. The vacuum pump and condenser maintained enough pressure for water permeation through the membrane. Alternatively, the driving force can be uncoupled when 2°C dew point air is recirculated as a sweeping air through the condenser as the vacuum pump controls the total system pressure [43]. According to the results, a WHR of 0.26 and 0.21 g min⁻¹ was potentially available at 32 and 10 L min⁻¹ airflow rates, respectively. The cooling of the recirculated sweep stream requires a smaller amount of energy as compared to the systems that produce water without membranes. However, a higher vapor loss rate was reported due to the reduction in permeate side pressure when the condenser was operating above the freezing point [43]. Additionally, Zhao et al. developed an air dehumidification cum AWH system using hollow fiber membranes, driven by a dry sweep stream with a vacuum pressure of 0.17 bars [44]. This system configuration saves energy up to 24.3% based on cooling 1 m³ of air and up to 38.9% based on producing 1 kg of potable water. Wu and coworkers proposed a novel electrospun, polyacrylonitrile (PAN) nanofibrous membrane with directional water transport capability for humidity harvesting, as illustrated in Fig. 6 [45]. This hydrophobic/hydrophilic directional-wicking membrane has the potential to enhance the water harvesting capability of existing membrane-assisted systems. The variation in pore sizes – smaller and larger pores in the hydrophilic and hydrophobic layers, respectively – improved water harvesting capacity by ~1.7 times [45]. Similarly, a polymeric electrolyte membrane (PEM) was developed for an electrochemical air dehumidification system having the potential to decrease humidity from 90% to less than 30% using a 3V electric field [46]. The moisture removal can be improved by increasing the humidity and air flow rates on the anode side. The main drawback of this system was the low coefficient of performance (COP≈0.33) as only 30% of the input power was used by the PEM element [46]. In the literature, reported power consumption (i.e., 0.16-0.19 kWh kg⁻¹) of membrane-assisted systems was relatively lower. However, the daily WHR was very small (i.e., 0.2 kg per day), due to the low air flow rate

(i.e., $0.84 \text{ m}^3 \text{ h}^{-1}$ on average) in their experiments. For membrane-assisted systems, the moisture transfer rate could be improved to become a competitive option for water vapors concentration [47].

Fig. 6 is inserted here.

2.4 Dew and Fog AWH

Dew and fog AWH are promising methods of passive cooling for water harvesting. Dew formation is a phase transition, naturally occurring phenomenon in which moisture in the atmosphere shifts its phase on solid surfaces which have a temperature below the dewpoint of the air [48,49]. The collection of dews can be considered as an atypical water source as it depends on the manipulation of natural processes. Passive dew harvesting has resulted a maximum WHR of 0.3 to 0.6 L m^{-2} per day [50]. For optimum WHR with the application of zero external energy, the physical properties like hydrophilic nature, size, position (inclination and orientation), and shape of the radiative condensers could be improved. Despite the improvements, weather condition influences the performance of the condenser and limits the applicability of this technique to regions with suitable environmental conditions, rendering it an unreliable source of AWH [50]. The energy consumption in dew collection is comparatively higher because of high energy input for overcoming latent heat of evaporation and for sub-dewpoint cooling of the air for AWH [51].

Fog particles are the micrometric droplets suspended in the atmosphere that grows in size by the surface tension action of water until they are large enough to be detached and collected by gravity [52]. The rate of fog harvesting is influenced by the psychrometric properties of the air i.e., absolute humidity, relative humidity, wind velocity, and fog frequency [52]. Fig. 7(a) illustrates a traditional mesh-collection method of fog. The fog droplets are trapped when the wind pushes the water droplets against the meshes in a foggy environment. A lightweight (80 kg at 12 m in height) warka water structure was reported in literature which consists of a polyester mesh inside a bamboo frame. In warka water structure, fog, rain, and dew particles grow larger colloids on the mesh and are subsequently collected [53]. Fig. 7(b) documents major milestones for fog water collection technology, many of which were inspired by mimicking the biological water-harvest mechanisms evolved for biospecies existing in an arid environment [54–58]. For example, the Namib desert beetle is a unique pattern in nature that collects water from fog to survive [56]. Table 2 summarizes the features in selected animals and plants facilitating water harvesting. Fig. 8 further shows the various technologies to fabricate bioinspired water harvesting materials. In short, fog water collection is a simple and inexpensive technology, albeit its reliance on climatological conditions makes water yield unpredictable. Low water productivity, as defined by the ratio of water collected at the sump and the liquid water flux normal to the mesh, has also been accentuated [54,59].

Fig. 7 is inserted here.

Fig. 8 is inserted here.

Table. 2 is inserted here.

2.5 Biomass gasification AWH

AWH as a byproduct of biomass gasification has been documented. One example is the downdraft gasifier and biomass-gasification-based AWH system which was feasible for water-deprived and agricultural regions, as shown in Fig. 9 [60]. This system leverages the heat energy generated from the combustion of biogas to its benefit by using it in the refrigeration system to condense water. This biomass gasification-based AWH system has a WHR rate of 0.8-1.2 mL kg⁻¹ of biomass. In conclusion, it was projected that this system, if fully deployed, could potentially meet the potable water needs of India up to 10-12%.

Fig. 9 is inserted here.

3 Principles and features of Adsorption-based AWH

In this section, the principles, and features of the adsorption-based AWH systems are discussed in detail, as are the water harvesting cycle during adsorption, desorption, and their performance. The psychrometric representation of a typical adsorption-based AWH system is also presented.

Adsorption-based AWH is a salient way of extracting water from the air as compared to fog harvesting and dewing because it can harvest water from air with a low moisture-harvesting index (MHI), thereby expanding the water harvesting capacity at a wider range of temperature and humidity level. Selective adsorbents or desiccants (i.e., metallic organic frameworks, zeolites, etc.) and their composites have been utilized in AWH systems [15,51,61,62]. Fig. 10 illustrates a typical adsorption-based AWH system consisting of an adsorbent layer, a condenser, and an enclosure space. The water harvesting cycle in the system comprises of (i) adsorption of water at night when adsorbents are in contact with low temperature and high RH ambient air, (ii) desorption of water during daytime when the adsorbents are in contact with high temperature, trapped air, and (iii) condensation of water vapors at a lower temperature. Fig. 11(a) shows the schematic of the basic adsorption-based AWH system that comprises a desiccant material for the adsorption and desorption processes along with a condenser. The psychrometric behavior of these AWH systems is also shown in Fig. 11(b). In the plot, point 1 represents the state of saturation of the adsorbent in a confined space, whereas point 2 represents the state of desorption of the adsorbent at a higher temperature, thus increasing humidity ratio. The atmospheric water is then collected at point 3 where water vapor changes into a liquid form. The adsorption and desorption kinetics of a desiccant material envisage the slope of the line joining points 1 and 2. The line connecting points 2 to 3 represents the condensation of air up to its dewpoint. The performance of such systems can be characterized by the following parameters: adsorption capacity per unit mass of adsorbents (Δx), relative pressure (RP), system's water harvesting capacity (M_{water}), recovery ratio (RR), specific energy consumption (SEC_{heat}), and heat for regenerated air (W_{heat}). The mathematical formulations of these parameters are given in Eq. (1)-(6) [63].

$$\Delta x = x_{ad}(T_{ad}, RP_{ad}) - x_{de}(T_{de}, RP_{de}) \quad (1)$$

$$RP = \frac{P_v}{P_{sat}(T_{sorber})} = RH \times \frac{P_{sat}(T_{air})}{P_{sat}(T_{sorber})} \quad (2)$$

$$M_{water} = p_{air,sorber} Q_{air,sorber} t_{sorber} (d_{desorber,o} - d_{cond}) \quad (3)$$

$$RR = \frac{M_{water}}{p_{air,sorber} Q_{air,sorber} t_{sorber} d_{sorber,i}} \approx \frac{d_{desorber,o} - d_{cond}}{d_{sorber,i}} \quad (4)$$

$$SEC_{heat} = \frac{W_{heat}}{M_{water}} = C_p \times \frac{T_{desorber,i} - T_{ambient}}{d_{desorber,o} - d_{cond}} \quad (5)$$

$$W_{heat} = C_p P_{air,desorber} Q_{air,desorber} t_{desorber} (T_{desorber,i} - T_{ambient}) \quad (6)$$

In these equations, $x_{ad}(T_{ad}, R_{ad})$ represents the adsorption curves and $x_{de}(T_{de}, R_{de})$ represents the desorption curves, p_v represents the partial pressure of water vapors, p_{sat} denotes the saturated vapor pressure, ρ denotes density, d_{cond} denotes the saturated humidity ratio, C_p denotes the specific heat capacity, whereas t_{sorber} and $t_{desorber}$ denote the periods of adsorption and desorption phases, respectively, and $d_{desorber,o}$ denote the moisture content of the desorber outlet air and $d_{sorber,i}$ shows the sorber inlet moisture content. The adsorbent materials are the essential components of any adsorption-based AWH system, either in solid or liquid form. Improvement in adsorbent materials leads to a significant amount of energy reduction in AWH systems. Generally, the adsorbents should fulfill the criteria such as flexibility in hydrophilicity, chemical stability, adjustable pore volume, sorption kinetics, crystal density, and stability in multiple water harvesting cycles [15]. The next section deals with the significance and selection of adsorbents that focus on water adsorption isotherms, adsorption kinetics, thermal conductivity, and thermophysical properties of some potential adsorbents for atmospheric water harvesting.

Fig. 10 is inserted here.

Fig. 11 is inserted here.

4 Recent developments in adsorbent materials for AWH

The performance of an adsorption-based AWH system is affected by the properties of the material (i.e., crystal size, adsorption uptake) and component (i.e., thermal conductivity, parasitic heat loss, vapor transport to a condenser) [51]. Many promising adsorbents have been proposed for AWH including silica gel, zeolites, metal-organic frameworks (MOFs), and other inorganic and organic materials of hygroscopic nature (e.g., CaCl_2 , LiCl) [15,26,64–69]. Silica gel granules and powders are among the most commonly used inorganic desiccants because they are economical and exhibit high stability, however, their AWH performance is limited due to less adsorption capacity [70–73]. Different hygroscopic salts (e.g., LiCl , MgSO_4) have been incorporated with silica gel to increase the adsorption capacity but the impregnation of hygroscopic salts results in corrosion, deliquescence, and spill-over which affects the application of these materials in adsorption based AWH [74–77]. Some aerogels are also inorganic desiccants and show high adsorption ability, but their application is restricted because of the requirement of high regeneration temperature [78]. Moreover, various substrates (e.g., hydrogel beads, metal foams) have been developed and used for AWH [61,64,66,79]. Materials that tend to deliquesce as they absorb moisture from humid air will result in limited AWH efficiency. Table 3 compiles the key features of moisture adsorbing materials for AWH reported in the literature. The different parameters such as water harvesting capacity, the energy required for desorption, stability under multiple cycles, and cost considerations greatly affect the selection of suitable adsorbents for AWH.

Table. 3 is inserted here.

4.1 Adsorption equilibrium/isotherms

The water adsorption uptake is one of the main features for adsorbents performance and a wealth of research has been conducted for common adsorbents such as silica gel [80,81], zeolite [82,83], activated alumina [84–86], polymeric and carbon-based adsorbents [87–90]. Despite the lack of standardized criteria for the selection of adsorbents, the consensus is that materials with a large maximum adsorption capacity for water molecules and characterized by Type IV or Type V (s-shaped) isotherms are the preferred choice for AWH. Herein, Fig. 12(a) shows the characteristic adsorption isotherms for moisture uptake [91], and Fig. 12(b) shows the recommended principles for MOF selection based on the capacity, isotherm shape, and stability in the adsorption and desorption cycles over repeated applications [15].

Fig. 12 is inserted here.

For the adsorbents to operate with these types of isotherms, a strong interaction is required with water molecules (capture), yet weak enough to release them (harvest) through temperature and pressure swing adsorption within the AWH cycle [92]. The gravimetric isotherm of adsorbents yields the equilibrium mass of water taken up in its maximum capability at the given temperature and relative humidity. The water adsorption isotherm is commonly described by the following parameters: (i) heat of adsorption (kJ mole^{-1}), (ii) adsorption capacity (g g^{-1}), (iii) K_H (slope of isotherm), and (iv) relative pressure α (inflection point of isotherm) [93]. The shape of adsorption isotherms can reveal important information about the adsorption dynamics and mechanisms. Fig. 13 shows the water adsorption isotherms of the various forms of microporous aluminophosphate zeolites (zeolite-13X, $\text{ALPO}_4\text{-34}$, $\text{ALPO}_4\text{-34}$, AQSOA-Z02). These zeolites have low regeneration temperature, and their adsorption is reversible and hydrothermally stable. Fig. 14 shows the water adsorption isotherms of several promising MOFs for AWH. MOFs have the advantage of being able to harvest more amount of water with a lower regeneration temperature when compared to other traditional adsorbents (e.g., silica gel, zeolite) [15]. The s-shaped isotherms of MOFs indicate that a very small change in RH or temperature can amplify into a marked difference in water uptake, resulting in an efficient operation in the water harvesting unit [94]. MOFs are structured forms of inorganic clusters linked by organic molecules [95]. A study reported the applicability of MOF-801 that can daily harvest the atmospheric water up to $\sim 2.8 \text{ L kg}^{-1}$ of MOF [67]. Lapotin and coworkers [51] investigated several different microporous zeolites which have a lower regeneration temperature (i.e., 75°C - 95°C). The results found that these zeolites have reversible adsorption, are hydrothermally stable, and are effective in water harvesting capacity (i.e., ~ 0.23 - 0.37 g g^{-1}). In addition, several highly porous, water-stable MOFs have been recently investigated, including MOF-801 [61], Ni-BTDD [96], Co-BTDD [96], and Al-fumarate [97]. The geometry, pore size, and chemical stability of these materials can be altered to tailor different applications. All these adsorbents exhibited a Type IV and Type V isotherm at low RH which makes them suitable for AWH.

Fig. 13 is inserted here.

Fig. 14 is inserted here.

4.2 Adsorption kinetics

Heat and mass transfer properties of adsorption-based AWH systems dictate their productivity and energy efficiency. The adsorbent's shape, crystal size, packing density, and porosity are among the primary factors for vapor transport in a packed-bed system [67,98,99]. Fig. 15 shows the material and component-level properties that govern the system's performance and efficiency. Intra-crystalline and inter-crystalline vapor diffusion, mass transport, and energy transfer in a packed-bed system can be calculated using Eq. (7-11) [51,98,100–105]

$$\frac{\partial C}{\partial t} = \frac{1}{r_c^2} \frac{\partial}{\partial r} \left(D_\mu r_c^2 \frac{\partial C}{\partial r} \right) \quad (7)$$

$$\frac{\partial C_\mu}{\partial t} = \frac{15}{r_c^2} D_\mu (C_{eq} - C_\mu) \quad (8)$$

$$D_v = \varepsilon^{3/2} \left(\frac{1}{D_{vap}} + \frac{1}{D_k} \right)^{-1} \quad (9)$$

$$\frac{\partial C}{\partial t} = \nabla \cdot D_v \nabla C - \frac{(1-\varepsilon)}{\varepsilon} \frac{\partial C_\mu}{\partial t} \quad (10)$$

$$\rho c_p \frac{\partial T}{\partial t} = \nabla \cdot k \nabla T + h_{ad} (1 - \varepsilon) \frac{\partial C_\mu}{\partial t} \quad (11)$$

In Eq. (7), C denotes the vapor concentration, D_μ represents the intracrystalline diffusivity, t denotes time, and r_c represents the spherical radius of the adsorbent. The intracrystalline diffusion can be determined by fitting Eq. (7) of Fick's law with the experimental data. Importantly, the intracrystalline diffusivity changes with different uptakes and temperatures, and therefore it is difficult to determine its values for various conditions. For that, it is necessary to define an average diffusivity for different conditions. With the averaged diffusivity, Eq. (8) will be used to model the adsorption kinetics. In Eq. (8), C_{eq} is the equilibrium vapor concentration and C_μ represents the instantaneous vapor concentration. Notably, radius influences the adsorption kinetics, as the smaller size crystals will take the adsorption kinetics more quickly and increase the resistance for inter-crystalline diffusion. Furthermore, the intercrystalline diffusion (i.e., water vapor diffusion) is a function of the particle shape, size, and packing density, and can be estimated by the modified Knudsen equation for tortuous media using Eq. (9) [105]. In Eq. (9), D_{vap} represents the vapor diffusivity in air and ε denotes the adsorbent porosity. Further, the mass transport and heat transfer for the adsorbent can be determined using Eq. (10) and Eq. (11). In Eq. (11), ρ denotes the average density, h_{ad} represents the adsorption enthalpy, c_p denotes the heat capacity, and k represents the thermal conductivity. These equations validate the experimental results and found that low packing densities severely limited the water vapor adsorption rate in a packed bed [106]. To attain faster adsorption kinetics, different zeolites such as X, Y, AQSOAZ01, and FAPO-34 have been used, but all of these require more than 100°C regeneration temperature [83,107].

Recently, various MOFs have been developed and utilized in AWH applications [61,94–96]. Table 4 summarizes some of the promising MOFs with high adsorption capacities. For AWH application, MOFs stability is critical that can be defined by the number of factors (i.e., linkers, porosity, metal ions, hydrophobicity). Fig. 16 graphically delineates the thermodynamics and kinetics of MOFs when applied for

reactions involving hydrolysis. It can be observed that the thermodynamic and kinetic stabilities are linked to Gibb's and activation energies, respectively. [15,108]. Several factors can render MOFs kinetic inertness as attributed to (i) steric hindrance of secondary building units (SBU), (ii) rigidity of SBUs, (iii) configuration of metal by electronically, (iv) hydrophobicity, and (v) steric hindrance through interpenetration [15]. Steric shielding (which can hinder the diffusion of water molecules to the metal centers) can be introduced in MOF structures in three ways; (i) catenation, (ii) SBUs with high-level linkage, and (iii) bulky linkers [15,109]. Importantly, increasing the MOF's water stability through hydrophobicity, restricts their water adsorption capability, particularly for AWH application which needs water adsorption at low relative pressures.

Fig. 15 is inserted here.

Fig. 16 is inserted here.

Table. 4 is inserted here.

4.3 Thermal Conductivity

The heat transfer efficiency of porous adsorbents can be lower because of low thermal conductivity. Moreover, low mass diffusivity and poor thermal conductivity of adsorbents also result in heavy and bulky adsorption systems [110,111]. The higher AWH capacity can be achieved for a specific adsorbent by improving the vapor and thermal transport rates. These concerns are especially important in the designing of modular beds, where it's typical to pack numerous layers, each with equal contact with moist air. Characteristically, improving one of these modes of transportation degrades the other. For instance, some conventional adsorption systems capitalize on the compaction of adsorbents to improve the thermal contact within the crystals, but this adversely impacts the vapor transport within the adsorbents. The consequences of developing sorbent-metallic fin composites have also been thoroughly investigated by the sorption heat pump community, but a considerable drop was noticed at micro and as well as at bulk scale vapor permeability. Additionally, the thermal mass of the system can be reduced with metal additives [112,113]. The use of zeolites merged with metallic foams has been investigated to increase the heat transfer phenomenon without affecting thermal mass [114]. By integrating thin coatings (~1 to 5 mm) of adsorbents with metallic substrates have been used as an alternative method for the reduction of heat resistance of sorbent beds. This method relies on decreasing the length of thermal transport and resistance among the adsorbent crystals. Such types of coatings for various desiccants (e.g., silica gel, MOFs, zeolites) have been developed with great success [115–117]. Another commonly-used technique is by dispersing a low mass percentage of highly thermally conductive material to enhance the thermal conductivity. The thermal conductivity of the composite adsorbents has been improved by the number of carbon-based materials, without changing the mass transfer properties [118]. For example, a carbon-based material (i.e., 2D few layers graphene) demonstrates excellent attributes in high thermal conductivity, high-temperature stability, and lower molecular weight. By increasing approx. 3 wt % of these enhancers, could improve the system's thermal conductivity by 25% [118]. Whereas several materials (i.e., graphene oxide, carbon nanotubes) did not perform well to enhance the thermal conductivity of composites because of poor thermal contact [118,119]. The potential downside of introducing

these additives is the additional vapor transport hindrance, created either by blocking the volume of pores or by reducing the inter-crystalline volume of voids. Therefore, the carbonaceous nanomaterial additives do not restrict vapor transport, particularly at low weight. The key task to select the pertinent adsorbent materials for AWH is to alter the forces among the materials and crystals of adsorbents to increase the contact area [118]. Table 5 compiles the thermal conductivity of some of the adsorbent materials. Notably, the composite adsorbents with expanded graphite possess high thermal conductivities [120–124]. To improve the thermal and vapor transfer simultaneously within the adsorbent material, a new 3-D graphene network material has been developed [125–127]. The newly developed zeolites and MOFs crammed within these graphene structures have shown improved thermal and vapor transfer rates attributed to the presence of micro-passages.

Table. 5 is inserted here.

5 Adsorption-based AWH systems and technologies

5.1 Solid desiccants-based AWH systems

Adsorption-based AWH can be done using desiccants (i.e., liquid, solid). Kumar et. al proposed a solar glass desiccant-based AWH system in which different desiccant materials (i.e., silica gel, CaCl_2 /saw wood, CaCl_2 /vermiculite/saw wood) were investigated [128–130]. A composite desiccant (CaCl_2 - saw wood) was developed and six samples were investigated with different concentrations (10%, 20%, 30%, 40%, 50%, 60%) of CaCl_2 in saw wood [128]. The results found that a sample (60% of CaCl_2) showed the WHR of 180 mL kg^{-1} per day. This maximum rate represents a water productivity that is 1.24, 1.63, 2.0, 2.57, and 2.76 times greater than those having 50%, 40%, 30%, 20%, and 10% CaCl_2 concentration, respectively. While silica gel showed the WHR of 200 mL kg^{-1} per day [129]. Further, a desiccant material (CaCl_2 /vermiculite/saw wood) was developed and showed the WHR of 195 mL kg^{-1} per day [130]. A combination of desiccant wheels and a VCC based system was developed for AWH [131]. In this system, the desiccant wheels were used for humidification of air, while the evaporator was utilized for dehumidification. With this approach, the WHR can be increased to a significant level. Fig. 17 shows the schematics of two scenarios of the proposed system. The major difference between both scenarios was that the heat exchanger cooled down the dehumidified air (A_{deh}) which was passing through the desiccant wheels as in Fig. 17 (a), while in the case of another scenario, the dehumidified air was changed with the ambient air as in Fig. 17 (b). Additionally, different patterns of heat pump systems were investigated. The results found that WHR of this system can be reached to 32.5 kg h^{-1} while the water harvesting efficiency (WHE) can be achieved to 1.26 kg kWh^{-1} .

Fig. 17 is inserted here.

A desiccant wheel dehumidifier-based prototype has been experimented with for AWH [132]. With this, a synthetic model was also built-in Transient System Simulation Tool (TRNSYS) which validated the experimental results. The inlet air was split up into two streams; the major stream went to the desiccant wheel while the minor stream passed through the heat exchanger to exchange the enthalpy with the regeneration stream to condense the water. When part of the desiccant wheel reached saturation condition, then it will ultimately attain the regeneration phase. A sufficient amount of heat was supplied through the hybrid solar

collectors to the air stream for regeneration purposes. The validated model was then run for various climatic conditions (i.e., Sydney, Abu Dhabi, and London) to simulate the annual WHR. The results showed that a silica gel desiccant wheel-based dehumidification system produced a WHR of a range of ~5.2 L per day of water in Sydney. Whereas the TRNSYS-simulated model predicts approximately 13.8, 18.5, and 10 kL of water in a year for Sydney, Abu Dhabi, and London, respectively. As described, many conventional porous materials (silica gel, zeolites, porous carbons) and other materials can extract enough water [133–136]. But all these materials suffer from major drawbacks such as low kinetics, low water uptake capacity, and high-water adsorption energy. Therefore, a new series of zirconium-based MOFs have been developed which showed extraordinary water uptake properties [137,138]. An adsorption-based AWH system was developed in which porous MOF-801 was used as a desiccant material [67]. Fig. 18 shows the pictorial representation of the proposed MOF-based AWH device along with the temperature, solar flux, and RH profiles. This prototype consists of a MOF-801 layer, an acrylic enclosure, and a low temperature condenser. It was noticed that a temperature swing of 40°C was enough to regenerate the MOF-801 and can harvest ~0.24 L kg⁻¹ of MOF per day. This prototype was successfully experienced in the climatic conditions of the Arizona desert after being tested on the roof of an institution [61]. Later on, MOF-801 based system was installed in the Arizona desert, which was composed of two boxes; one for MOF, and the other box was equipped with a cover [69]. The cover lid was open at night for an adsorption phase while it was closed during the night for the desorption phase. After the experiments, it was concluded that ~200-300 mL kg⁻¹ of MOF per day can be achieved at ambient conditions of range 20-40°C and 5-40% RH. This device was proved as the first breakthrough to harvest drinkable atmospheric water from the desert air.

Fig. 18 is inserted here.

MOF-303 based AWH system was developed which was capable of performing continuous and multiple water harvesting cycles per day [69,139]. The advantage of MOF-303 is that it is composed of SBUs and can harvest drinking water even at low RH. This device was first tested at the parent university, where it showed a WHR of 1.3 L kg⁻¹ per day at conditions of 32% RH and 27°C. Then this system was experimentally experienced in the Mojave Desert, where it showed an extraordinary performance with WHR of 0.7 L kg⁻¹ per day at conditions of 10% RH and 27°C. After analysis, it was concluded that this second-generation MOF-303 based AWH system showed 10 times perfection as compared to other systems due to rod-like SBUs of MOF-303 which makes it more stable over many cycles. Moreover, the highly open structure of MOF-303 makes it more suitable in both adsorption and desorption phases. Logan et al. investigated different hydrolytically stable MOFs to explore the adsorption/desorption kinetics for AWH and found MOF-808 can achieve the WHR of ~8.6 L kg⁻¹ of MOF per day [140]. MOFs have emerged as the most favorable adsorbents for AWH because of their reticular chemistry. Some of the important features of reticular chemistry include hydrolytic stability, step-shaped isotherm profile, iso-reticular expansion, ultra-high uptake, SBU modification, and linker functionality [141]. Further, AWH through composite desiccants represented some extraordinary results. Ji et al. fabricated and tested a small solar-driven AWH unit in which MCM-41/CaCl₂ was utilized as a composite desiccant [142]. The developed system produced about ~1.2 kg of water per collector area. Wang et al. developed and tested two solar-driven devices (i.e., concept machine, and semi-open) in which the composite desiccants (i.e., ACF-LiCl,

ACF-CaCl₂) were used for AWH [143]. Fig. 19 and Fig. 20 show the schematics of solar-driven AWH devices. The performance psychrometric charts of the concept and improved solar-driven devices consist of four main points in a cycle. ACF-CaCl₂ was rolled up in a concept machine while, in an improved device, the corrugated and flat layers of the ACF matrix with LiCl were placed layer by layer. The results found that the concept machine-generated water about ~0.3 kg with 2.3 kg of composite material (ACF-CaCl₂). Meanwhile, the improved semi-open type of solar-driven device produced water about ~9 kg with 40.8 kg of composite material (ACF-LiCl).

Fig. 19 is inserted here.

Fig. 20 is inserted here.

Entezari et al. investigated the ACF material as a host of different hygroscopic salts (i.e., LiCl, CaCl₂, and LiNO₃) for AWH [144]. The proposed prototype consists of two chambers, one is an upper chamber with an aluminum sheet roof and the other is a lower chamber with a condenser. A hydrophobic polysiloxane layer was utilized at the bottom of the upper chamber to make the system perform in all considered RH. The results found that this prototype can produce about 1.5 g g⁻¹ of desiccant at 70% RH. Ejeian et al. designed and developed a prototype in which a new composite material (i.e., LiCl/MgSO₄/ACF) was investigated for AWH. The results showed that it can produce about 0.9 g g⁻¹ of desiccant at 35% RH and found an appropriate choice for AWH especially in the areas of moderate relative humidity [145]. Wang et al. prepared different composite materials with varying concentrations of matrices and salts and named as SCCA, SCLI, ASCA, ASLI, ECA, ELI, ESCA, and ESLI [66]. The results found that the composite ACF performs much better than the pure ACF in terms of sorption and desorption (i.e., ~0.6 g g⁻¹ at conditions of 20% RH and 77°C). A clean water harvester was developed in which a new composite material (i.e., sodium polyacrylate graphene framework) was investigated which efficiently grabs the water vapors and releases enough amount of water [146]. Fig. 21 shows the concept of PGF along with the developed system. The results showed the WHR of 25 L kg⁻¹ of material per day.

Fig. 21 is inserted here.

5.2 Liquid desiccants-based AWH systems

AWH based on desiccant materials (solid, liquid) performs adsorption/ absorption phenomenon during nighttime and desorption phenomenon during daytime. Liquid desiccant materials appear to offer additional benefits i.e., higher moisture retention than solid desiccants. Furthermore, liquid desiccants require lower regeneration temperatures, ranging from 40°C to 70°C [147]. Researchers investigated different liquid desiccants impregnated with various substances (i.e., cloth, and sand) to enhance water productivity [148–150]. In this context, an absorption-regeneration cycle of the AWH system was modified by the sultan and coworkers [151], which was first suggested by Hamed [152]. The modified cycle is composed of four processes: isothermal absorption, heating of absorbent, isothermal regeneration, and cooling of absorbent. A solar thermal driven experimental system was developed and tested at Mansoura University, Egypt for AWH in which CaCl₂ was used as a desiccant material shown in Fig. 22 [153]. During the nighttime, the finned type of absorber is

subjected to the atmosphere for absorption of water vapors. Whereas at day time, the finned type of absorber is tightly covered with a cone type surface and directly exposed to the sun for desorption of water vapors. The vapor pressure difference between the desiccant material and the surface of the cover causes the water vapors to evaporate and condense. The system showed the WHR of 0.63 kg m^{-2} per day with an efficiency ranging from 11.26% to 22.56%. The portable AWH can be possible using this system.

Fig. 22 is inserted here.

Another solar-driven based AWH system was developed and investigated in the Helwan University, Cairo-Egypt in which CaCl_2 was used as a desiccant material [154]. Fig. 23 shows the schematic and visual representation of the developed system with the variation of total evaporated mass, system efficiency, and total collected water. The system was tested in summer conditions with different materials and the results showed that the evaporated water for cloth bed was 870 g m^{-2} per day in September while, in the case for sand bed, it was 310 g m^{-2} per day. Moreover, in humid conditions, efficiency of 16.5% and total water of 1200 g m^{-2} per day was noted for cloth bed. The six-layers bed showed 10.4% more efficiency as compared to the four-layers bed and the system efficiencies were 4.8% and 5.9% for areal densities of 10 and 12 kg m^{-2} for sand bed. Hamed and coworkers investigated a CaCl_2 desiccant solution-based AWH system in the cities of Al-Hada and Taif in Saudi Arabia. Average freshwater productivity of 1 g m^{-2} per day was obtained using this system [155].

Fig. 23 is inserted here.

A liquid desiccant-based humidification-dehumidification (HDH) system for AWH was proposed and investigated [156]. The proposed HDH system produced water at WHR of 8 kg h^{-1} capacity in which the desiccant solution was used as a mist to the humidifier, thus outlet air then losses the absorbed moisture as freshwater. Because of the mass and heat transfer between the air and desiccant solution, the thermodynamic balancing of such systems becomes necessary to minimize entropy generation [157]. After several studies, multi-stage HDH systems were considered, the most thermodynamically balanced systems [158]. The “enthalpy pinch” was introduced to investigate both heat and mass exchange because the “temperature pinch” method could not considered appropriate to make thermodynamically balanced systems [159]. Till now, water-based HDH systems have been the main subject of investigation. Fig. 24(a) shows the schematic of the HDH system for AWH [156]. The proposed HDH system was upgraded with air dryers and multiple extractions for thermodynamic balancing. LiCl_2 was used as a desiccant solution for AWH. To compare between five extractions, the 1 kJ kg_a^{-1} of enthalpy pinch was selected, whereas 20 kJ kg_a^{-1} was chosen at typical operating conditions for one extraction. The system performance was analyzed by gained output ratio (GOR) and the relation of enthalpy pinch with GOR is presented in Fig. 24(b). The results found that GOR varies with the number of extractions. Additionally, energy consumption also decreases as the number of extractions increases shown in Fig. 24(b). As the air dryers increase, the WHR was also increased as in Fig. 24(c). Guido et al. developed a liquid desiccant-based AWH system in which pure water vapors were condensed to collect the freshwater [160]. Fig. 25(a) shows the proposed system in which the operation of system was modeled by ABSorption SIMulation (ABSIM) software for thermodynamic analysis [161]. LiCl_2 was used as a desiccant

solution for AWH. In ABSIM modeling, the range of temperatures (7°C to 35°C) and mixing ratios (i.e., $0.006\text{ kg}_w\text{ kg}_a^{-1}$ to $0.024\text{ kg}_w\text{ kg}_a^{-1}$) were investigated. This system can be operated with electrical energy or by a low-temperature heat source. Fig. 25(b) shows the WHR against the various ambient conditions and the optimum temperatures of the cold and hot streams (necessary for desorber and condenser) are presented in Fig. 25(c) and Fig. 25(d). The modeling results were compared with locally AWH systems and observed that it can save up to 5% to 65% of the energy requirements because of the mechanism of separation process. The condensation temperature ranges from 4°C to 15°C varies under different ambient conditions. The proposed vapor separation technology showed a great potential for AWH because of the quality of produced water and energy consumption.

Fig. 24 is inserted here.

Fig. 25 is inserted here.

6 Future of adsorption based AWH systems/technologies

The adsorption-based AWH systems have attained so much attention as an environmentally friendly option in recent years, but unfortunately, they could not establish themselves as a commercial technology. The main reasons include the lack of knowledge and related fundamental studies about AWH technology among the designers, developers, industrialists, and end-users. Table 6 shows the comparison among the various approaches for AWH according to the costs of construction, maintenance, operation, and environmental effects. It is difficult to install an adsorption-based AWH system in those regions where thermal energy is reluctantly available because its performance mainly relies on the regeneration of desiccant material. Therefore, the thermal energy-based system should be designed and developed in the foreseeable future. Research and development have become a vital program across the globe and have been increased in the field of AWH with the development of novel materials and modifications in hydrophilic and hydrophobic properties. However, future research should pay attention on the desorption process and number of adsorption/desorption cycles in more detail. The researchers pursued several ways to improve systems efficiencies by providing novel desiccant materials, especially in low RH conditions. The number of adsorbent materials has been explored in literature due to their unique structures such as MOFs, zeolites, and various composite adsorbents. But all studies have one similar theme: they only paid attention to the adsorption uptakes of desiccant materials and overlook other essential parameters like adsorption kinetics. The kinetics and transport of the desiccant materials directly affect the adsorption-based AWH system's effectiveness, and size. Tu et al. presented two innovative designs for improvement in energy efficiencies and reduction in systems size [17]. Fig. 26(a) shows water heated desiccant-coated heat exchanger-based system which has a conceivable potential to collect the water vapors because water cooling adsorption and condensation were applied to enhance the RR of feed air and to reduce the SEC of the system. Similarly, Fig. 26(b) shows the configuration of a desiccant-based heat pump system which is best possible for those areas where continuous AWH is required. It is evident from this review paper that research towards developing and commercializing energy-efficient and environmentally friendly adsorption-based AWH systems is well in progress.

Fig. 26 is inserted here.

Table. 6 is inserted here.

7 Conclusions

The present study addresses the current prospects and challenges of various AWH technologies and is categorized into active cooling i.e., vapor compression, thermoelectric cooling, and membrane-based AWH, and passive cooling i.e., dew collection and fog harvesting. Throughout the literature, it has been found that these technologies possess some limits of climate dependency and cost considerations to deliver enough amount of water. However, the adsorption-based AWH technologies emerged as an attractive option to harvest water from air anywhere and anytime. Therefore, this work compiles a comprehensive review on adsorption-based AWH technologies/ systems, and consequently the adsorption equilibrium/isotherms and kinetics, and thermal conductivity of desiccant materials are discussed with reference literature. It has been found that the adsorption-based AWH systems performed much better as compared to other AWH technologies. Among the considered zeolites, maximum equilibrium uptake was found for $\text{ALPO}_4\text{-LTA}$, i.e., 0.4 g g^{-1} . In addition, the Cr-soc-MOF-1 showed an equilibrium uptake of 1.8 g g^{-1} while (Cr) MIL-101 showed the maximum equilibrium uptake of 1.4 g g^{-1} . It has been concluded that the MOFs are advantageous compared to other desiccant materials as they harvest more amount of water and require lower regeneration temperatures. MOF-801 showed an equilibrium uptake of 0.3 g g^{-1} and delivered $200\text{-}300 \text{ mL kg}^{-1}$ of water at $5\text{-}40\% \text{ RH}$ and $20\text{-}40^\circ\text{C}$ and proved as a potential candidate for AWH. Moreover, Zr-MOF-808 showed an AWH capacity of $8.66 \text{ L kg}^{-1} \text{ d}^{-1}$. Similarly, the harvesting capacities of CaCl_2 and LiCl -based AWH systems were found in between 0.63 to $1.0 \text{ kg m}^{-2} \text{ d}^{-1}$. The reference studies show that the adsorption-based AWH technologies have received a lot of attention as an environmentally friendly option but could not succeed to appear as a commercial technology due to lack of knowledge among the designers, developers, industrialists, and end-users.

Declarations of interest

There are no interests to declare.

CRedit authorship contribution statement

Muhammad Bilal: Conceptualization, Methodology, Software, Formal analysis, Investigation, Writing – Original Draft. **Muhammad Sultan:** Conceptualization, Methodology, Validation, Resources, Writing – Original Draft, Visualization, Supervision, Project administration, Funding acquisition. **Tatiana Morosuk:** Investigation, Validation, Resources, Writing – Review & Editing, Supervision, Project administration, Funding acquisition. **Walter Den:** Formal analysis, Investigation, Writing – Review & Editing, Visualization. **Uzair Sajjad:** Data Curation, Wiring – Review & Editing, Visualization. **Mian MA Aslam:** Writing – Review & Editing, Visualization. **Muhammad W. Shahzad:** Formal analysis, Validation, Writing – Review & Editing, Visualization. **Muhammad Farooq:** Data Curation, Investigation, Writing – Review & Editing, Visualization.

Acknowledgments

This research was carried out in the Department of Agricultural Engineering, Bahauddin Zakariya University, Multan-Pakistan. The authors acknowledge the financial support from Bahauddin Zakariya University under the research grant of ORIC Project# 2020-21, awarded to Principal Investigator Dr. Muhammad Sultan.

References

- [1] du Plessis A. Water as a Source of Conflict and Global Risk. Water as an Inescapable Risk, Springer; 2019, p. 115–43. https://doi.org/10.1007/978-3-030-03186-2_6.
- [2] Wang L, d'Odorico P, Evans JP, Eldridge DJ, McCabe MF, Caylor KK, et al. Dryland ecohydrology and climate change: critical issues and technical advances 2012.
- [3] Beysens D. Dew water. River Publishers; 2018.
- [4] Lee M, Keller AA, Chiang P-C, Den W, Wang H, Hou C-H, et al. Water-energy nexus for urban water systems: A comparative review on energy intensity and environmental impacts in relation to global water risks. Appl Energy 2017;205:589–601. <https://doi.org/10.1016/j.apenergy.2017.08.002>.
- [5] Oelkers EH, Hering JG, Zhu C. Water: Is There a Global Crisis? Elements 2011;7:157–62. <https://doi.org/10.2113/gselements.7.3.157>.
- [6] Shiklomanov IA. World fresh water resources. Water in Crisis: A Guide to the World's Fresh Water Resources 1993:379–82.
- [7] Mekonnen MM, Hoekstra AY. Four billion people facing severe water scarcity. Sci Adv 2016;2:e1500323. <https://doi.org/10.1126/sciadv.1500323>.
- [8] Den W, Chen C-H, Luo Y-C. Revisiting the water-use efficiency performance for microelectronics manufacturing facilities: Using Taiwan's Science Parks as a case study. Water-Energy Nexus 2018;1:116–33. <https://doi.org/10.1016/j.wen.2018.12.002>.
- [9] United Nations. Sustainable Development Goal 6 synthesis report on water and sanitation. vol. 10017. 2018.
- [10] Ligtoet W, Hilderink H. Towards a world of cities in 2050 An outlook on water- related challenges - Background report to the UN-Habitat Global Report. 2014.
- [11] Elimelech M, Phillip WA. The Future of Seawater Desalination: Energy, Technology, and the Environment. Science (80-) 2011;333:712–7. <https://doi.org/10.1126/science.1200488>.
- [12] Hamdy S, Morosuk T, Tsatsaronis G. Exergoeconomic optimization of an adiabatic cryogenics-based energy storage system. Energy 2019;183:812–24. <https://doi.org/10.1016/j.energy.2019.06.176>.
- [13] Riaz N, Sultan M, Miyazaki T, Shahzad MW, Farooq M, Sajjad U, et al. A review of recent advances in adsorption desalination technologies. Int Commun Heat Mass Transf 2021;128:105594. <https://doi.org/10.1016/j.icheatmasstransfer.2021.105594>.
- [14] Wahlgren R V. Atmospheric water vapour processor designs for potable water production: a review. Water Res 2001;35:1–22. [https://doi.org/10.1016/S0043-1354\(00\)00247-5](https://doi.org/10.1016/S0043-1354(00)00247-5).
- [15] Kalmutzki MJ, Diercks CS, Yaghi OM. Metal–Organic Frameworks for Water Harvesting from Air. Adv Mater 2018;30:1–26. <https://doi.org/10.1002/adma.201704304>.
- [16] Carotenuto A, Fucci F, La Fianza G. Adsorption phenomena in porous media in presence of moist air.

Int Commun Heat Mass Transf 1991;18:71–81. [https://doi.org/https://doi.org/10.1016/0735-1933\(91\)90009-S](https://doi.org/https://doi.org/10.1016/0735-1933(91)90009-S).

[17] Tu Y, Wang R, Zhang Y, Wang J. Progress and Expectation of Atmospheric Water Harvesting. *Joule* 2018;2:1452–75. <https://doi.org/10.1016/j.joule.2018.07.015>.

[18] Kim H, Rao SR, LaPotin A, Lee S, Wang EN. Thermodynamic analysis and optimization of adsorption-based atmospheric water harvesting. *Int J Heat Mass Transf* 2020;161:120253. <https://doi.org/10.1016/j.ijheatmasstransfer.2020.120253>.

[19] Ejeian M, Wang RZ. Adsorption-based atmospheric water harvesting. *Joule* 2021;5:1678–703. <https://doi.org/10.1016/j.joule.2021.04.005>.

[20] Zhou X, Lu H, Zhao F, Yu G. Atmospheric Water Harvesting: A Review of Material and Structural Designs. *ACS Mater Lett* 2020;2:671–84. <https://doi.org/10.1021/acsmaterialslett.0c00130>.

[21] Sultan M, Bilal M, Miyazaki T, Sajjad U, Ahmad F. Adsorption-Based Atmospheric Water Harvesting: Technology Fundamentals and Energy-Efficient Adsorbents. In: Ahmad F, Sultan M, editors. *Technol. Agric.*, United Kingdom: IntechOpen; 2021. <https://doi.org/10.5772/intechopen.97301>.

[22] Kobayashi M. A method of obtaining water in arid lands. *Sol Energy* 1963;7:93–9. [https://doi.org/10.1016/0038-092X\(63\)90034-3](https://doi.org/10.1016/0038-092X(63)90034-3).

[23] Hall RC. Theoretical calculations on the production of water from the atmosphere by absorption with subsequent recovery in a solar still. *Sol Energy* 1966;10:41–5. [https://doi.org/10.1016/0038-092X\(66\)90071-5](https://doi.org/10.1016/0038-092X(66)90071-5).

[24] Sofrata H. Non-conventional system for water collection. In *Proceedings of solar desalination workshop*. vol. 2, 1981, p. 71–87.

[25] Alayli Y, Hadji NE, Leblond J. A new process for the extraction of water from air. *Desalination* 1987;67:227–9.

[26] Gordeeva LG, Tokarev MM, Parmon VN, Aristov YI. Selective water sorbents for multiple application, 6. Freshwater production from the atmosphere. *React Kinet Catal Lett* 1998;65:153–9.

[27] Morosuk T, Sultan M. Low-temperature Technologies. IntechOpen; 2020. <https://doi.org/10.5772/intechopen.78524>.

[28] Dalkilic AS, Wongwises S. A performance comparison of vapour-compression refrigeration system using various alternative refrigerants. *Int Commun Heat Mass Transf* 2010;37:1340–9. <https://doi.org/https://doi.org/10.1016/j.icheatmasstransfer.2010.07.006>.

[29] Luo J, Zhang W, Bai X. Development and application of a field water maker. *J HV&AC* 2004;34:42–5.

[30] Zolfagharkhani S, Zamen M, Shahmardan MM. Thermodynamic analysis and evaluation of a gas compression refrigeration cycle for fresh water production from atmospheric air. *Energy Convers Manag* 2018;170:97–107. <https://doi.org/10.1016/j.enconman.2018.05.016>.

[31] Talib AJ, Khalifa AHN, Mohammed AQ. Performance study of water harvesting unit working under iraqi conditions. *Int J Air-Conditioning Refrig* 2019;27. <https://doi.org/10.1142/S2010132519500111>.

[32] Granryd E. Hydrocarbons as refrigerants — an overview. *Int J Refrig* 2001;24:15–24. [https://doi.org/10.1016/S0140-7007\(00\)00065-7](https://doi.org/10.1016/S0140-7007(00)00065-7).

[33] Calm JM. The next generation of refrigerants – Historical review, considerations, and outlook. *Int J Refrig* 2008;31:1123–33. <https://doi.org/10.1016/j.ijrefrig.2008.01.013>.

719 [34] Mussati SF, Morosuk T, Mussati MC. Superstructure-Based Optimization of Vapor Compression-
720 Absorption Cascade Refrigeration Systems. *Entropy* 2020;22:428. <https://doi.org/10.3390/e22040428>.

721 [35] Tashtoush B, Younes MB. Comparative thermodynamic study of refrigerants to select the best
722 environment-friendly refrigerant for use in a solar ejector cooling system. *Arab J Sci Eng*
723 2019;44:1165–84.

724 [36] Sadati SE, Rahbar N, Kargarsharifabad H, KhalesiDoost A. Low thermal conductivity measurement
725 using thermoelectric technology - Mathematical modeling and experimental analysis. *Int Commun Heat*
726 *Mass Transf* 2021;127:105534. <https://doi.org/https://doi.org/10.1016/j.icheatmasstransfer.2021.105534>.

727 [37] Zhang T, Wan RH, Yan T, Wang L, Lin CH. Development of Portable Air-based Water Collector for
728 Field Operations under Conditions of Severe Water Shortage. *Chinese Med Equip J* 2010;31:70–2.

729 [38] Cao D, Zou Y. System Optimization of Water Exaction from Air by Semiconductor Cooling Air [J].
730 *Build Energy Environ* 2016;35:71–3.

731 [39] Atta RM. Solar water condensation using thermoelectric coolers. *Int J Water Resour Arid Environ*
732 2011;1:142–5.

733 [40] Eslami M, Tajeddini F, Etaati N. Thermal analysis and optimization of a system for water harvesting
734 from humid air using thermoelectric coolers. *Energy Convers Manag* 2018;174:417–29.
735 <https://doi.org/10.1016/j.enconman.2018.08.045>.

736 [41] Morosuk T, Tsatsaronis G. Advanced exergetic evaluation of refrigeration machines using different
737 working fluids. *Energy* 2009;34:2248–58. <https://doi.org/10.1016/j.energy.2009.01.006>.

738 [42] Bergmair D, Metz SJ, De Lange HC, van Steenhoven AA. System analysis of membrane facilitated
739 water generation from air humidity. *Desalination* 2014;339:26–33.
740 <https://doi.org/10.1016/j.desal.2014.02.007>.

741 [43] Bergmair D, Metz SJ, De Lange HC, Van Steenhoven AA. A low pressure recirculated sweep stream
742 for energy efficient membrane facilitated humidity harvesting. *Sep Purif Technol* 2015;150:112–8.
743 <https://doi.org/10.1016/j.seppur.2015.06.042>.

744 [44] Zhao B, Wang LY, Chung TS. Enhanced membrane systems to harvest water and provide comfortable
745 air via dehumidification & moisture condensation. *Sep Purif Technol* 2019;220:136–44.
746 <https://doi.org/10.1016/j.seppur.2019.03.034>.

747 [45] Wu J, Zhou H, Wang H, Shao H, Yan G, Lin T. Novel Water Harvesting Fibrous Membranes with
748 Directional Water Transport Capability. *Adv Mater Interfaces* 2019;6:1–9.
749 <https://doi.org/10.1002/admi.201801529>.

750 [46] Qi R, Li D, Zhang LZ. Performance investigation on polymeric electrolyte membrane-based
751 electrochemical air dehumidification system. *Appl Energy* 2017;208:1174–83.
752 <https://doi.org/10.1016/j.apenergy.2017.09.035>.

753 [47] Tu R, Hwang Y. Reviews of atmospheric water harvesting technologies. *Energy* 2020;201:117630.
754 <https://doi.org/10.1016/j.energy.2020.117630>.

755 [48] Agam N, Berliner PR. Dew formation and water vapor adsorption in semi-arid environments—A
756 review. *J Arid Environ* 2006;65:572–90. <https://doi.org/https://doi.org/10.1016/j.jaridenv.2005.09.004>.

757 [49] Beysens D. The formation of dew. *Atmos Res* 1995;39:215–37. [https://doi.org/10.1016/0169-](https://doi.org/10.1016/0169-8095(95)00015-J)
758 8095(95)00015-J.

- [50] Khalil B, Adamowski J, Shabbir A, Jang C, Rojas M, Reilly K, et al. A review: dew water collection from radiative passive collectors to recent developments of active collectors. *Sustain Water Resour Manag* 2016;2:71–86. <https://doi.org/10.1007/s40899-015-0038-z>.
- [51] LaPotin A, Kim H, Rao SR, Wang EN. Adsorption-Based Atmospheric Water Harvesting: Impact of Material and Component Properties on System-Level Performance. *Acc Chem Res* 2019;52:1588–97. <https://doi.org/10.1021/acs.accounts.9b00062>.
- [52] Cáceres L, Gómez-Silva B, Garró X, Rodríguez V, Monardes V, McKay CP. Relative humidity patterns and fog water precipitation in the Atacama Desert and biological implications. *J Geophys Res Biogeosciences* 2007;112.
- [53] Hobson B. Arturo Vittori's Warka Water towers harvest clean drinking water from the air 2016. <https://www.dezeen.com/>.
- [54] Park KC, Chhatre SS, Srinivasan S, Cohen RE, McKinley GH. Optimal design of permeable fiber network structures for fog harvesting. *Langmuir* 2013;29:13269–77. <https://doi.org/10.1021/la402409f>.
- [55] Zheng Y, Bai H, Huang Z, Tian X, Nie FQ, Zhao Y, et al. Directional water collection on wetted spider silk. *Nature* 2010;463:640–3. <https://doi.org/10.1038/nature08729>.
- [56] Bai H, Wang L, Ju J, Sun R, Zheng Y, Jiang L. Efficient water collection on integrative bioinspired surfaces with star-shaped wettability patterns. *Adv Mater* 2014;26:5025–30. <https://doi.org/10.1002/adma.201400262>.
- [57] Nørgaard T, Dacke M. Fog-basking behaviour and water collection efficiency in Namib Desert Darkling beetles. *Front Zool* 2010;7:1–8. <https://doi.org/10.1186/1742-9994-7-23>.
- [58] Liu C, Xue Y, Chen Y, Zheng Y. Effective directional self-gathering of drops on spine of cactus with splayed capillary arrays. *Sci Rep* 2015;5:1–8. <https://doi.org/10.1038/srep17757>.
- [59] Montecinos S, Carvajal D, Cereceda P, Concha M. Collection efficiency of fog events. *Atmos Res* 2018;209:163–9. <https://doi.org/10.1016/j.atmosres.2018.04.004>.
- [60] Chaitanya B, Bahadur V, Thakur AD, Raj R. Biomass-gasification-based atmospheric water harvesting in India. *Energy* 2018;165:610–21. <https://doi.org/10.1016/j.energy.2018.09.183>.
- [61] Kim H, Rao SR, Kapustin EA, Zhao L, Yang S, Yaghi OM, et al. Adsorption-based atmospheric water harvesting device for arid climates. *Nat Commun* 2018;9:1–8. <https://doi.org/10.1038/s41467-018-03162-7>.
- [62] Wang JY, Liu JY, Wang RZ, Wang LW. Experimental investigation on two solar-driven sorption based devices to extract fresh water from atmosphere. *Appl Therm Eng* 2017;127:1608–16. <https://doi.org/10.1016/j.applthermaleng.2017.09.063>.
- [63] Wang JY, Wang RZ, Tu YD, Wang LW. Universal scalable sorption-based atmosphere water harvesting. *Energy* 2018;165:387–95. <https://doi.org/10.1016/j.energy.2018.09.106>.
- [64] Kallenberger PA, Fröba M. Water harvesting from air with a hygroscopic salt in a hydrogel-derived matrix. *Commun Chem* 2018;1:6–11. <https://doi.org/10.1038/s42004-018-0028-9>.
- [65] Elmer TH, Hyde JF. Recovery of Water from Atmospheric Air in Arid Climates. *Sep Sci Technol* 1986;21:251–66. <https://doi.org/10.1080/01496398608058376>.
- [66] Wang JY, Liu JY, Wang RZ, Wang LW. Experimental research of composite solid sorbents for fresh water production driven by solar energy. *Appl Therm Eng* 2017;121:941–50.

799 <https://doi.org/10.1016/j.applthermaleng.2017.04.161>.

800 [67] Kim H, Yang S, Rao SR, Narayanan S, Kapustin EA, Furukawa H, et al. Water harvesting from air with
801 metal-organic frameworks powered by natural sunlight. *Science* (80-) 2017;356:430.
802 <https://doi.org/10.1126/science.aam8743>.

803 [68] Yang, SuKim H, Rao SR, Narayanan S, Kapustin EA, Furukawa H, Umans AS, et al. Powered By
804 Natural Sunlight. *Science* (80-) 2017;434:430–4. <https://doi.org/10.1126/science.aam8743>.

805 [69] Fathieh F, Kalmutzki MJ, Kapustin EA, Waller PJ, Yang J, Yaghi OM. Practical water production from
806 desert air. *Sci Adv* 2018;4:1–10. <https://doi.org/10.1126/sciadv.aat3198>.

807 [70] Li A, Thu K, Ismail A Bin, Shahzad MW, Ng KC. Performance of adsorbent-embedded heat exchangers
808 using binder-coating method. *Int J Heat Mass Transf* 2016;92:149–57.

809 [71] Zhao Y, Ge TS, Dai YJ, Wang RZ. Experimental investigation on a desiccant dehumidification unit
810 using fin-tube heat exchanger with silica gel coating. *Appl Therm Eng* 2014;63:52–8.

811 [72] Ismail A Bin, Li A, Thu K, Ng KC, Chun W. On the thermodynamics of refrigerant+ heterogeneous
812 solid surfaces adsorption. *Langmuir* 2013;29:14494–502.

813 [73] Ge TS, Dai YJ, Wang RZ, Peng ZZ. Experimental comparison and analysis on silica gel and polymer
814 coated fin-tube heat exchangers. *Energy* 2010;35:2893–900.

815 [74] Jiang Y, Ge TS, Wang RZ, Hu LM. Experimental investigation and analysis of composite silica-gel
816 coated fin-tube heat exchangers. *Int J Refrig* 2015;51:169–79.

817 [75] Gordeeva LG, Restuccia G, Cacciola G, Aristov YI. Selective water sorbents for multiple applications,
818 5. LiBr confined in mesopores of silica gel: sorption properties. *React Kinet Catal Lett* 1998;63:81–8.

819 [76] Leiming H, Tianshu G, Yu J, Ruzhu W. Hygroscopic property of metal matrix composite desiccant. *J*
820 *Refrig* 2014;2:12.

821 [77] Simonova IA, Freni A, Restuccia G, Aristov YI. Water sorption on composite “silica modified by
822 calcium nitrate.” *Microporous Mesoporous Mater* 2009;122:223–8.

823 [78] Dorcheh AS, Abbasi MH. Silica aerogel synthesis, properties and characterization. *J Mater Process*
824 *Technol* 2008;199:10–26.

825 [79] Kabeel AE. Application of sandy bed solar collector system for water extraction from air. *Int J Energy*
826 *Res* 2006;30:381–94. <https://doi.org/10.1002/er.1155>.

827 [80] Xia ZZ, Chen CJ, Kiplagat JK, Wang RZ, Hu JQ. Adsorption Equilibrium of Water on Silica Gel. *J*
828 *Chem Eng Data* 2008;53:2462–5. <https://doi.org/10.1021/je800019u>.

829 [81] Chua HT, Ng KC, Chakraborty A, Oo NM, Othman MA. Adsorption Characteristics of Silica Gel +
830 Water Systems. *J Chem Eng Data* 2002;47:1177–81. <https://doi.org/10.1021/je0255067>.

831 [82] Wang Y, LeVan MD. Adsorption equilibrium of carbon dioxide and water vapor on zeolites 5A and
832 13X and silica gel: pure components. *J Chem Eng Data* 2009;54:2839–44.

833 [83] Kim J-H, Lee C-H, Kim W-S, Lee J-S, Kim J-T, Suh J-K, et al. Adsorption equilibria of water vapor on
834 alumina, zeolite 13X, and a zeolite X/activated carbon composite. *J Chem Eng Data* 2003;48:137–41.

835 [84] Abd-Elrahman WR, Hamed AM, El-Emam SH, Awad MM. Experimental investigation on the
836 performance of radial flow desiccant bed using activated alumina. *Appl Therm Eng* 2011;31:2709–15.

837 [85] Serbezov A. Adsorption equilibrium of water vapor on F-200 activated alumina. *J Chem Eng Data*
838 2003;48:421–5.

- [86] Ruthven DM, Hussain M, Desai R. Adsorption of water vapour on activated alumina. *Stud. Surf. Sci. Catal.*, vol. 80, Elsevier; 1993, p. 545–52.
- [87] Do DD, Junpirom S, Do HD. A new adsorption–desorption model for water adsorption in activated carbon. *Carbon N Y* 2009;47:1466–73.
- [88] Sultan M, El-Sharkawy II, Miyazaki T, Saha BB, Koyama S. Experimental study on carbon based adsorbents for greenhouse dehumidification. *Evergr Jt J Nov Carbon Resour Sci Green Asia Strat* 2014;1.
- [89] Toribio F, Bellat JP, Nguyen PH, Dupont M. Adsorption of water vapor by poly (styrenesulfonic acid), sodium salt: isothermal and isobaric adsorption equilibria. *J Colloid Interface Sci* 2004;280:315–21.
- [90] Sultan M, Miyazaki T, Koyama S, Khan ZM. Performance evaluation of hydrophilic organic polymer sorbents for desiccant air-conditioning applications. *Adsorpt Sci Technol* 2018;36:311–26. <https://doi.org/10.1177/0263617417692338>.
- [91] Sing KSW. Reporting physisorption data for gas/solid systems with special reference to the determination of surface area and porosity (Recommendations 1984). *Pure Appl Chem* 1985;57:603–19.
- [92] Ashraf S, Sultan M, Bahrami M, McCague C, Shahzad MW, Amani M, et al. Recent progress on water vapor adsorption equilibrium by metal-organic frameworks for heat transformation applications. *Int Commun Heat Mass Transf* 2021;124:105242. <https://doi.org/https://doi.org/10.1016/j.icheatmasstransfer.2021.105242>.
- [93] Canivet J, Bonnefoy J, Daniel C, Legrand A, Coasne B, Farrusseng D. Structure–property relationships of water adsorption in metal–organic frameworks. *New J Chem* 2014;38:3102–11.
- [94] De Lange MF, Verouden KJFM, Vlugt TJH, Gascon J, Kapteijn F. Adsorption-Driven Heat Pumps: The Potential of Metal–Organic Frameworks. *Chem Rev* 2015;115:12205–50. <https://doi.org/10.1021/acs.chemrev.5b00059>.
- [95] Canivet J, Fateeva A, Guo Y, Coasne B, Farrusseng D. Water adsorption in MOFs: fundamentals and applications. *Chem Soc Rev* 2014;43:5594–617.
- [96] Rieth AJ, Yang S, Wang EN, Dincă M. Record atmospheric fresh water capture and heat transfer with a material operating at the water uptake reversibility limit. *ACS Cent Sci* 2017;3:668–72.
- [97] Teo HWB, Chakraborty A, Kitagawa Y, Kayal S. Experimental study of isotherms and kinetics for adsorption of water on Aluminium Fumarate. *Int J Heat Mass Transf* 2017;114:621–7.
- [98] Narayanan S, Yang S, Kim H, Wang EN. Optimization of adsorption processes for climate control and thermal energy storage. *Int J Heat Mass Transf* 2014;77:288–300.
- [99] Wan A, Yang J, Chen T, Huang J. Techno-economic analysis of combined cycle power plant with waste heat-driven adsorption inlet air cooling system. *Int Commun Heat Mass Transf* 2021;126:105422. <https://doi.org/https://doi.org/10.1016/j.icheatmasstransfer.2021.105422>.
- [100] Narayanan S, Kim H, Umans A, Yang S, Li X, Schiffres SN, et al. A thermophysical battery for storage-based climate control. *Appl Energy* 2017;189:31–43.
- [101] Sircar S, Hufton JR. Why does the linear driving force model for adsorption kinetics work? *Adsorption* 2000;6:137–47. <https://doi.org/10.1023/A:1008965317983>.
- [102] Alonso M, Sainz E, Lopez FA, Shinohara K. Void-size probability distribution in random packings of equal-sized spheres. *Chem Eng Sci* 1995;50:1983–8.

- 879 [103] Chan KC, Chao CYH, Sze-To GN, Hui KS. Performance predictions for a new zeolite 13X/CaCl₂
880 composite adsorbent for adsorption cooling systems. *Int J Heat Mass Transf* 2012;55:3214–24.
- 881 [104] Moldrup P, Olesen T, Gamst J, Schjønning P, Yamaguchi T, Rolston DE. Predicting the gas diffusion
882 coefficient in repacked soil water-induced linear reduction model. *Soil Sci Soc Am J* 2000;64:1588–94.
- 883 [105] Marshall TJ. The diffusion of gases through porous media. *J Soil Sci* 1959;10:79–82.
- 884 [106] Zheng X, Wang RZ, Ge TS. Experimental study and performance predication of carbon based
885 composite desiccants for desiccant coated heat exchangers. *Int J Refrig* 2016;72:124–31.
- 886 [107] Teo HWB, Chakraborty A, Fan W. Improved adsorption characteristics data for AQSOA types zeolites
887 and water systems under static and dynamic conditions. *Microporous Mesoporous Mater* 2017;242:109–
888 17.
- 889 [108] Liu X, Wang X, Kapteijn F. Water and Metal-Organic Frameworks: From Interaction toward
890 Utilization. *Chem Rev* 2020. <https://doi.org/10.1021/acs.chemrev.9b00746>.
- 891 [109] Azmi WH, Hamid KA, Usri NA, Mamat R, Sharma K V. Heat transfer augmentation of ethylene glycol:
892 water nanofluids and applications — A review. *Int Commun Heat Mass Transf* 2016;75:13–23.
893 <https://doi.org/https://doi.org/10.1016/j.icheatmasstransfer.2016.03.018>.
- 894 [110] Sultan M, El-Sharkawy II, Miyazaki T, Saha BB, Koyama S, Maruyama T, et al. Insights of water vapor
895 sorption onto polymer based sorbents. *Adsorption* 2015;21:205–15.
- 896 [111] Kazemi I, Sefid M, Afrand M. Improving the thermal conductivity of water by adding mono & hybrid
897 nano-additives containing graphene and silica: A comparative experimental study. *Int Commun Heat*
898 *Mass Transf* 2020;116:104648. <https://doi.org/https://doi.org/10.1016/j.icheatmasstransfer.2020.104648>.
- 899 [112] Narayanan S, Li X, Kim H, Umans A, Wang EN. RECENT ADVANCES IN ADSORPTION-BASED
900 HEATING AND COOLING SYSTEMS. *Annu Rev Heat Transf* 2016;19:199–239.
901 <https://doi.org/10.1615/AnnualRevHeatTransfer.2016015440>.
- 902 [113] Gu J, Bart H-J. Heat and mass transfer in steam desorption of an activated carbon adsorber. *Int Commun*
903 *Heat Mass Transf* 2005;32:296–304.
904 <https://doi.org/https://doi.org/10.1016/j.icheatmasstransfer.2004.07.002>.
- 905 [114] Groll M. Reaction beds for dry sorption machines. *Heat Recover Syst CHP* 1993;13:341–6.
906 [https://doi.org/10.1016/0890-4332\(93\)90059-5](https://doi.org/10.1016/0890-4332(93)90059-5).
- 907 [115] Jeremias F, Henninger SK, Janiak C. High performance metal–organic-framework coatings obtained via
908 thermal gradient synthesis. *Chem Commun* 2012;48:9708. <https://doi.org/10.1039/c2cc34782b>.
- 909 [116] Bonaccorsi L, Calabrese L, Freni A, Proverbio E, Restuccia G. Zeolites direct synthesis on heat
910 exchangers for adsorption heat pumps. *Appl Therm Eng* 2013;50:1590–5.
911 <https://doi.org/10.1016/j.applthermaleng.2011.10.028>.
- 912 [117] Jiang Y, Dehghan S, Karimipour A, Toghraie D, Li Z, Tlili I. Effect of copper nanoparticles on thermal
913 behavior of water flow in a zig-zag nanochannel using molecular dynamics simulation. *Int Commun*
914 *Heat Mass Transf* 2020;116:104652.
915 <https://doi.org/https://doi.org/10.1016/j.icheatmasstransfer.2020.104652>.
- 916 [118] Yang S, Kim H, Narayanan S, McKay IS, Wang EN. Dimensionality effects of carbon-based thermal
917 additives for microporous adsorbents. *Mater Des* 2015;85:520–6.
- 918 [119] Yang S, Huang X, Chen G, Wang EN. Three-dimensional graphene enhanced heat conduction of porous

crystals. *J Porous Mater* 2016;23:1647–52. <https://doi.org/10.1007/s10934-016-0225-9>.

[120] Pons M, Laurent D, Meunier F. Experimental temperature fronts for adsorptive heat pump applications. *Appl Therm Eng* 1996;16:395–404.

[121] Mauran S, Prades P, L'haridon F. Heat and mass transfer in consolidated reacting beds for thermochemical systems. *Heat Recover Syst CHP* 1993;13:315–9.

[122] Eun T-H, Song H-K, Han JH, Lee K-H, Kim J-N. Enhancement of heat and mass transfer in silica-expanded graphite composite blocks for adsorption heat pumps: Part I. Characterization of the composite blocks. *Int J Refrig* 2000;23:64–73.

[123] Eun T-H, Song H-K, Han JH, Lee K-H, Kim J-N. Enhancement of heat and mass transfer in silica-expanded graphite composite blocks for adsorption heat pumps. Part II. Cooling system using the composite blocks. *Int J Refrig* 2000;23:74–81.

[124] Zheng X, Wang LW, Wang RZ, Ge TS, Ishugah TF. Thermal conductivity, pore structure and adsorption performance of compact composite silica gel. *Int J Heat Mass Transf* 2014;68:435–43.

[125] McKay IS, Yang S, Wang EN, Kim H. Percolated microstructures for multi-modal transport enhancement in porous active materials 2018.

[126] Giwa SO, Sharifpur M, Meyer JP. Experimental investigation into heat transfer performance of water-based magnetic hybrid nanofluids in a rectangular cavity exposed to magnetic excitation. *Int Commun Heat Mass Transf* 2020;116:104698. <https://doi.org/https://doi.org/10.1016/j.icheatmasstransfer.2020.104698>.

[127] Zhang FF, Li XY, Chen G, Wang T, Jin TX, Cheng CX, et al. Thermophysical properties and water sorption characteristics of 1-ethyl-3-methylimidazolium acetate ionic liquid and water binary systems. *Int Commun Heat Mass Transf* 2021;127:105558. <https://doi.org/https://doi.org/10.1016/j.icheatmasstransfer.2021.105558>.

[128] Kumar M, Yadav A. Experimental investigation of solar powered water production from atmospheric air by using composite desiccant material “CaCl₂/saw wood.” *Desalination* 2015;367:216–22.

[129] Kumar M, Yadav A. Experimental investigation of design parameters of solar glass desiccant box type system for water production from atmospheric air. *J Renew Sustain Energy* 2015;7. <https://doi.org/10.1063/1.4922142>.

[130] Kumar M, Yadav A. Composite desiccant material “CaCl₂/Vermiculite/Saw wood”: a new material for fresh water production from atmospheric air. *Appl Water Sci* 2017;7:2103–11.

[131] Tu R, Hwang Y. Performance analyses of a new system for water harvesting from moist air that combines multi-stage desiccant wheels and vapor compression cycles. *Energy Convers Manag* 2019;198:111811. <https://doi.org/10.1016/j.enconman.2019.111811>.

[132] Milani D, Qadir A, Vassallo A, Chiesa M, Abbas A. Experimentally validated model for atmospheric water generation using a solar assisted desiccant dehumidification system. *Energy Build* 2014;77:236–46. <https://doi.org/10.1016/j.enbuild.2014.03.041>.

[133] Yu N, Wang RZ, Lu ZS, Wang LW. Development and characterization of silica gel–LiCl composite sorbents for thermal energy storage. *Chem Eng Sci* 2014;111:73–84.

[134] Ng E-P, Mintova S. Nanoporous materials with enhanced hydrophilicity and high water sorption capacity. *Microporous Mesoporous Mater* 2008;114:1–26.

- 959 [135] Krajnc A, Varlec J, Mazaj M, Ristić A, Logar NZ, Mali G. Superior Performance of Microporous
 960 Aluminophosphate with LTA Topology in Solar-Energy Storage and Heat Reallocation. *Adv Energy*
 961 *Mater* 2017;7:1601815.
- 962 [136] Zhong W, He T, Hardick S, Trojanowski R, Butcher T, Wagner T, et al. Experiments of active polymer
 963 thermosyphons for water harvesting applications. *Int. Heat Transf. Conf. Digit. Libr.*, Begel House Inc.;
 964 2018.
- 965 [137] Furukawa H, Gándara F, Zhang YB, Jiang J, Queen WL, Hudson MR, et al. Water adsorption in porous
 966 metal-organic frameworks and related materials. *J Am Chem Soc* 2014;136:4369–81.
 967 <https://doi.org/10.1021/ja500330a>.
- 968 [138] Xu W, Yaghi OM. Metal – Organic Frameworks for Water Harvesting from Air, Anywhere, Anytime
 969 2020. <https://doi.org/10.1021/acscentsci.0c00678>.
- 970 [139] Hanikel N, Prévot MS, Fathieh F, Kapustin EA, Lyu H, Wang H, et al. Rapid Cycling and Exceptional
 971 Yield in a Metal-Organic Framework Water Harvester. *ACS Cent Sci* 2019;5:1699–706.
 972 <https://doi.org/10.1021/acscentsci.9b00745>.
- 973 [140] Logan MW, Langevin S, Xia Z. Reversible Atmospheric Water Harvesting Using Metal-Organic
 974 Frameworks. *Sci Rep* 2020;10:1–11. <https://doi.org/10.1038/s41598-020-58405-9>.
- 975 [141] Hanikel N, Prévot MS, Yaghi OM. MOF water harvesters. *Nat Nanotechnol* 2020;15:348–55.
 976 <https://doi.org/10.1038/s41565-020-0673-x>.
- 977 [142] Ji JG, Wang RZ, Li LX. New composite adsorbent for solar-driven fresh water production from the
 978 atmosphere. *Desalination* 2007;212:176–82. <https://doi.org/10.1016/j.desal.2006.10.008>.
- 979 [143] Wang JY, Wang RZ, Wang LW. Water vapor sorption performance of ACF-CaCl₂ and silica gel-CaCl₂
 980 composite adsorbents. *Appl Therm Eng* 2016;100:893–901.
 981 <https://doi.org/10.1016/j.applthermaleng.2016.02.100>.
- 982 [144] Entezari A, Ejeian M, Wang RZ. Extraordinary air water harvesting performance with three phase
 983 sorption. *Mater Today Energy* 2019;13:362–73. <https://doi.org/10.1016/j.mtener.2019.07.001>.
- 984 [145] Ejeian M, Entezari A, Wang RZ. Solar powered atmospheric water harvesting with enhanced LiCl
 985 /MgSO₄/ACF composite. *Appl Therm Eng* 2020;176:115396.
 986 <https://doi.org/10.1016/j.applthermaleng.2020.115396>.
- 987 [146] Yao H, Zhang P, Huang Y, Cheng H, Li C, Qu L. Highly Efficient Clean Water Production from
 988 Contaminated Air with a Wide Humidity Range. *Adv Mater* 2020;32:1–8.
 989 <https://doi.org/10.1002/adma.201905875>.
- 990 [147] Katejanekarn T, Chirarattananon S, Kumar S. An experimental study of a solar-regenerated liquid
 991 desiccant ventilation pre-conditioning system. *Sol Energy* 2009;83:920–33.
 992 <https://doi.org/10.1016/j.solener.2008.12.006>.
- 993 [148] Gad H., Hamed A., El-Sharkawy I. Application of a solar desiccant/collector system for water recovery
 994 from atmospheric air. *Renew Energy* 2001;22:541–56. [https://doi.org/10.1016/S0960-1481\(00\)00112-9](https://doi.org/10.1016/S0960-1481(00)00112-9).
- 995 [149] Abualhamayel HI, Gandhidasan P. A method of obtaining fresh water from the humid atmosphere.
 996 *Desalination* 1997;113:51–63. [https://doi.org/10.1016/S0011-9164\(97\)00114-8](https://doi.org/10.1016/S0011-9164(97)00114-8).
- 997 [150] Hamed AM. Experimental investigation on the natural absorption on the surface of sandy layer
 998 impregnated with liquid desiccant. *Renew Energy* 2003;28:1587–96. <https://doi.org/10.1016/S0960->

999 1481(03)00005-3.

1000 [151] Sultan A. Absorption/regeneration non-conventional system for water extraction from atmospheric air.
 1001 Renew Energy 2004;29:1515–35. [https://doi.org/10.1016/S0960-1481\(03\)00020-X](https://doi.org/10.1016/S0960-1481(03)00020-X).

1002 [152] Hamed AM. Absorption–regeneration cycle for production of water from air-theoretical approach.
 1003 Renew Energy 2000;19:625–35. [https://doi.org/10.1016/S0960-1481\(99\)00068-3](https://doi.org/10.1016/S0960-1481(99)00068-3).

1004 [153] Talaat MA, Awad MM, Zeidan EB, Hamed AM. Solar-powered portable apparatus for extracting water
 1005 from air using desiccant solution. Renew Energy 2018;119:662–74.
 1006 <https://doi.org/10.1016/j.renene.2017.12.050>.

1007 [154] William GE, Mohamed MH, Fatouh M. Desiccant system for water production from humid air using
 1008 solar energy. Energy 2015;90:1707–20. <https://doi.org/10.1016/j.energy.2015.06.125>.

1009 [155] Hamed AM, Aly AA, Zeidan E-SB. Application of solar energy for recovery of water from atmospheric
 1010 air in climatic zones of Saudi Arabia. Nat Resour 2011;2:8.

1011 [156] Ahmed MA, Zubair SM, Abido MA, Bahaidarah HM. An innovative closed-air closed-desiccant HDH
 1012 system to extract water from the air: A case for zero-brine discharge system. Desalination
 1013 2018;445:236–48.

1014 [157] Thiel GP, McGovern RK, Zubair SM, Lienhard V JH. Thermodynamic equipartition for increased
 1015 second law efficiency. Appl Energy 2014;118:292–9. <https://doi.org/10.1016/j.apenergy.2013.12.033>.

1016 [158] Zamen M, Soufari SM, Amidpour M. Improvement of solar humidification-dehumidification
 1017 desalination using multi-stage process. Chem Eng 2011;25.

1018 [159] Narayan GP, Chehayeb KM, McGovern RK, Thiel GP, Zubair SM. Thermodynamic balancing of the
 1019 humidification dehumidification desalination system by mass extraction and injection. Int J Heat Mass
 1020 Transf 2013;57:756–70.

1021 [160] Gido B, Friedler E, Broday DM. Liquid-Desiccant Vapor Separation Reduces the Energy Requirements
 1022 of Atmospheric Moisture Harvesting. Environ Sci Technol 2016;50:8362–7.
 1023 <https://doi.org/10.1021/acs.est.6b01280>.

1024 [161] Grossman G, Zaltash A. ABSIM—modular simulation of advanced absorption systems. Int J Refrig
 1025 2001;24:531–43.

1026 [162] Salehi AA, Ghannadi-Maragheh M, Torab-Mostaedi M, Torkaman R, Asadollahzadeh M. A review on
 1027 the water-energy nexus for drinking water production from humid air. Renew Sustain Energy Rev
 1028 2020;120:109627. <https://doi.org/10.1016/j.rser.2019.109627>.

1029 [163] Fessehaye M, Abdul-Wahab SA, Savage MJ, Kohler T, Gherezghiher T, Hurni H. Fog-water collection
 1030 for community use. Renew Sustain Energy Rev 2014;29:52–62.
 1031 <https://doi.org/10.1016/j.rser.2013.08.063>.

1032 [164] Zhang S, Huang J, Chen Z, Lai Y. Bioinspired Special Wettability Surfaces: From Fundamental
 1033 Research to Water Harvesting Applications. Small 2017;13. <https://doi.org/10.1002/smll.201602992>.

1034 [165] Sultan M, Miyazaki T, Koyama S. Optimization of adsorption isotherm types for desiccant air-
 1035 conditioning applications. Renew Energy 2018;121:441–50.
 1036 <https://doi.org/10.1016/j.renene.2018.01.045>.

1037 [166] Kayal S, Baichuan S, Saha BB. Adsorption characteristics of AQSOA zeolites and water for adsorption
 1038 chillers. Int J Heat Mass Transf 2016;92:1120–7.

- 1039 [167] Kim S-I, Yoon T-U, Kim M-B, Lee S-J, Hwang YK, Chang J-S, et al. Metal–organic frameworks with
1040 high working capacities and cyclic hydrothermal stabilities for fresh water production. *Chem Eng J*
1041 2016;286:467–75. <https://doi.org/http://dx.doi.org/10.1016/j.cej.2015.10.098>.
- 1042 [168] De Lange MF, Gutierrez-Sevillano J-J, Hamad S, Vlught TJH, Calero S, Gascon J, et al. Understanding
1043 adsorption of highly polar vapors on mesoporous MIL-100 (Cr) and MIL-101 (Cr): experiments and
1044 molecular simulations. *J Phys Chem C* 2013;117:7613–22.
- 1045 [169] Towsif Abtab SM, Alezi D, Bhatt PM, Shkurenko A, Belmabkhout Y, Aggarwal H, et al. Reticular
1046 Chemistry in Action: A Hydrolytically Stable MOF Capturing Twice Its Weight in Adsorbed Water.
1047 *Chem* 2018;4:94–105. <https://doi.org/10.1016/j.chempr.2017.11.005>.
- 1048 [170] Qasem NAA, Ahmed MA, Zubair SM. The impact of thermodynamic balancing on performance of a
1049 desiccant-based humidification-dehumidification system to harvest freshwater from atmospheric air.
1050 *Energy Convers Manag* 2019;199:112011. <https://doi.org/10.1016/j.enconman.2019.112011>.
- 1051 [171] Yang LT. Study of refrigeration system on water production through cooling air. *Tianjin Univ Commer*
1052 2013.
- 1053 [172] Muñoz-García MA, Moreda GP, Raga-Arroyo MP, Marín-González O. Water harvesting for young
1054 trees using Peltier modules powered by photovoltaic solar energy. *Comput Electron Agric* 2013;93:60–
1055 7.
- 1056 [173] Liu S, He W, Hu D, Lv S, Chen D, Wu X, et al. Experimental analysis of a portable atmospheric water
1057 generator by thermoelectric cooling method. *Energy Procedia* 2017;142:1609–14.
- 1058 [174] Brown PS, Bhushan B. Bioinspired materials for water supply and management: Water collection, water
1059 purification and separation of water from oil. *Philos Trans R Soc A Math Phys Eng Sci* 2016;374.
1060 <https://doi.org/10.1098/rsta.2016.0135>.
- 1061 [175] Parker AR, Lawrence CR. Water capture by a desert beetle. *Nature* 2001;414:33–4.
1062 <https://doi.org/10.1038/35102108>.
- 1063 [176] Bentley PJ, Blumer WFC. Uptake of water by the lizard, *Moloch horridus*. *Nature* 1962;194:699–700.
- 1064 [177] Sherbrooke WC, Scardino AJ, de Nys R, Schwarzkopf L. Functional morphology of scale hinges used
1065 to transport water: convergent drinking adaptations in desert lizards (*Moloch horridus* and *Phrynosoma*
1066 *cornutum*). *Zoomorphology* 2007;126:89–102.
- 1067 [178] Ju J, Bai H, Zheng Y, Zhao T, Fang R, Jiang L. A multi-structural and multi-functional integrated fog
1068 collection system in cactus. *Nat Commun* 2012;3:1–6. <https://doi.org/10.1038/ncomms2253>.
- 1069 [179] Roth-Nebelsick A, Ebner M, Miranda T, Gottschalk V, Voigt D, Gorb S, et al. Leaf surface structures
1070 enable the endemic Namib desert grass *Stipagrostis sabulicola* to irrigate itself with fog water. *J R Soc*
1071 *Interface* 2012;9:1965–74. <https://doi.org/10.1098/rsif.2011.0847>.
- 1072 [180] Aristov YI, Tokarev MM, Gordeeva LG, Snytnikov VN, Parmon VN. New composite sorbents for
1073 solar-driven technology of fresh water production from the atmosphere. *Sol Energy* 1999;66:165–8.
- 1074 [181] Elnaby KA. Water recovery from atmospheric air using wick desiccant solar still. *Environ Eng Manag J*
1075 2015;14:2365–72.
- 1076 [182] Tso CY, Chao CYH. Activated carbon, silica-gel and calcium chloride composite adsorbents for energy
1077 efficient solar adsorption cooling and dehumidification systems. *Int J Refrig* 2012;35:1626–38.
- 1078 [183] Srivastava S, Yadav A. Water generation from atmospheric air by using composite desiccant material

1079 through fixed focus concentrating solar thermal power. *Sol Energy* 2018;169:302–15.

1080 [184] Wang JY, Wang RZ, Wang LW, Liu JY. A high efficient semi-open system for fresh water production
1081 from atmosphere. *Energy* 2017;138:542–51. <https://doi.org/10.1016/j.energy.2017.07.106>.

1082 [185] Li R, Shi Y, Wu M, Hong S, Wang P. Improving atmospheric water production yield: Enabling multiple
1083 water harvesting cycles with nano sorbent. *Nano Energy* 2020;67:104255.

1084 [186] Li R, Shi Y, Shi L, Alsaedi M, Wang P. Harvesting water from air: using anhydrous salt with sunlight.
1085 *Environ Sci Technol* 2018;52:5398–406.

1086 [187] Gordeeva LG, Restuccia G, Freni A, Aristov YI. Water sorption on composites “LiBr in a porous
1087 carbon.” *Fuel Process Technol* 2002;79:225–31.

1088 [188] Nandakumar DK, Zhang Y, Ravi SK, Guo N, Zhang C, Tan SC. Solar energy triggered clean water
1089 harvesting from humid air existing above sea surface enabled by a hydrogel with ultrahigh
1090 hygroscopicity. *Adv Mater* 2019;31:1806730.

1091 [189] Ahnfeldt T, Guillou N, Gunzelmann D, Margiolaki I, Loiseau T, Férey G, et al. [Al₄(OH)₂(OCH₃)₄
1092 (H₂N-bdc)₃]_n·x H₂O: A 12-Connected Porous Metal–Organic Framework with an Unprecedented
1093 Aluminum-Containing Brick. *Angew Chemie Int Ed* 2009;48:5163–6.

1094 [190] AbdulHalim RG, Bhatt PM, Belmabkhout Y, Shkurenko A, Adil K, Barbour LJ, et al. A fine-tuned
1095 metal–organic framework for autonomous indoor moisture control. *J Am Chem Soc* 2017;139:10715–
1096 22.

1097 [191] Ko N, Hong J, Sung S, Cordova KE, Park HJ, Yang JK, et al. A significant enhancement of water
1098 vapour uptake at low pressure by amine-functionalization of UiO-67. *Dalt Trans* 2015;44:2047–51.

1099 [192] Cai G, Jiang H. A Modulator-Induced Defect-Formation Strategy to Hierarchically Porous Metal–
1100 Organic Frameworks with High Stability. *Angew Chemie Int Ed* 2017;56:563–7.

1101 [193] Cadiau A, Lee JS, Damasceno Borges D, Fabry P, Devic T, Wharmby MT, et al. Design of Hydrophilic
1102 Metal Organic Framework Water Adsorbents for Heat Reallocation. *Adv Mater* 2015;27:4775–80.
1103 <https://doi.org/10.1002/adma.201502418>.

1104 [194] De Lange MF, Zeng T, Vlught TJH, Gascon J, Kapteijn F. Manufacture of dense CAU-10-H coatings for
1105 application in adsorption driven heat pumps: optimization and characterization. *CrystEngComm*
1106 2015;17:5911–20.

1107 [195] Reinsch H, van der Veen MA, Gil B, Marszalek B, Verbiest T, de Vos D, et al. Structures, Sorption
1108 Characteristics, and Nonlinear Optical Properties of a New Series of Highly Stable Aluminum MOFs.
1109 *Chem Mater* 2013;25:17–26. <https://doi.org/10.1021/cm3025445>.

1110 [196] Wiersum AD, Soubeyrand-Lenoir E, Yang Q, Moulin B, Guillerme V, Yahia M Ben, et al. An evaluation
1111 of UiO-66 for gas-based applications. *Chem Asian J* 2011;6:3270–80.

1112 [197] Kandiah M, Nilsen MH, Usseglio S, Jakobsen S, Olsbye U, Tilset M, et al. Synthesis and Stability of
1113 Tagged UiO-66 Zr-MOFs. *Chem Mater* 2010;22:6632–40. <https://doi.org/10.1021/cm102601v>.

1114 [198] Jeremias F, Fröhlich D, Janiak C, Henninger SK. Advancement of sorption-based heat transformation
1115 by a metal coating of highly-stable, hydrophilic aluminium fumarate MOF. *RSC Adv* 2014;4:24073–82.
1116 <https://doi.org/10.1039/C4RA03794D>.

1117 [199] Wang S, Lee JS, Wahiduzzaman M, Park J, Muschi M, Martineau-Corcus C, et al. A robust large-pore
1118 zirconium carboxylate metal–organic framework for energy-efficient water-sorption-driven

1119 refrigeration. *Nat Energy* 2018;3:985–93.

1120 [200] Bjurström H, Karawacki E, Carlsson B. Thermal conductivity of a microporous particulate medium:
 1121 moist silica gel. *Int J Heat Mass Transf* 1984;27:2025–36.

1122 [201] Fayazmanesh K, McCague C, Bahrami M. Consolidated adsorbent containing graphite flakes for heat-
 1123 driven water sorption cooling systems. *Appl Therm Eng* 2017;123:753–60.

1124 [202] Tanashev YY, Aristov YI. Thermal conductivity of a silica gel+ calcium chloride system: the effect of
 1125 adsorbed water. *J Eng Phys Thermophys* 2000;73:876–83.

1126 [203] Wittstadt U, Földner G, Andersen O, Herrmann R, Schmidt F. A new adsorbent composite material
 1127 based on metal fiber technology and its application in adsorption heat exchangers. *Energies*
 1128 2015;8:8431–46.

1129 [204] Okamoto K, Teduka M, Nakano T, Kubokawa S, Kakiuchi H. The development of AQSOA water vapor
 1130 adsorbent and AQSOA coated heat exchanger. *Proc. Int. Symp. Innov. Mater. Process. Energy Syst.*
 1131 (IMPRESS 2010), Singapore, vol. 29, 2010, p. 2732.

1132 [205] N'Tsoukpoe KE, Restuccia G, Schmidt T, Py X. The size of sorbents in low pressure sorption or
 1133 thermochemical energy storage processes. *Energy* 2014;77:983–98.

1134 [206] Tamainot-Telto Z, Critoph RE. Monolithic carbon for sorption refrigeration and heat pump applications.
 1135 *Appl Therm Eng* 2001;21:37–52.

1136 [207] Huang BL, Ni Z, Millward A, McGaughey AJH, Uher C, Kaviani M, et al. Thermal conductivity of a
 1137 metal-organic framework (MOF-5): Part II. Measurement. *Int J Heat Mass Transf* 2007;50:405–11.
 1138 <https://doi.org/10.1016/j.ijheatmasstransfer.2006.10.001>.

1139

1140

List of Figures

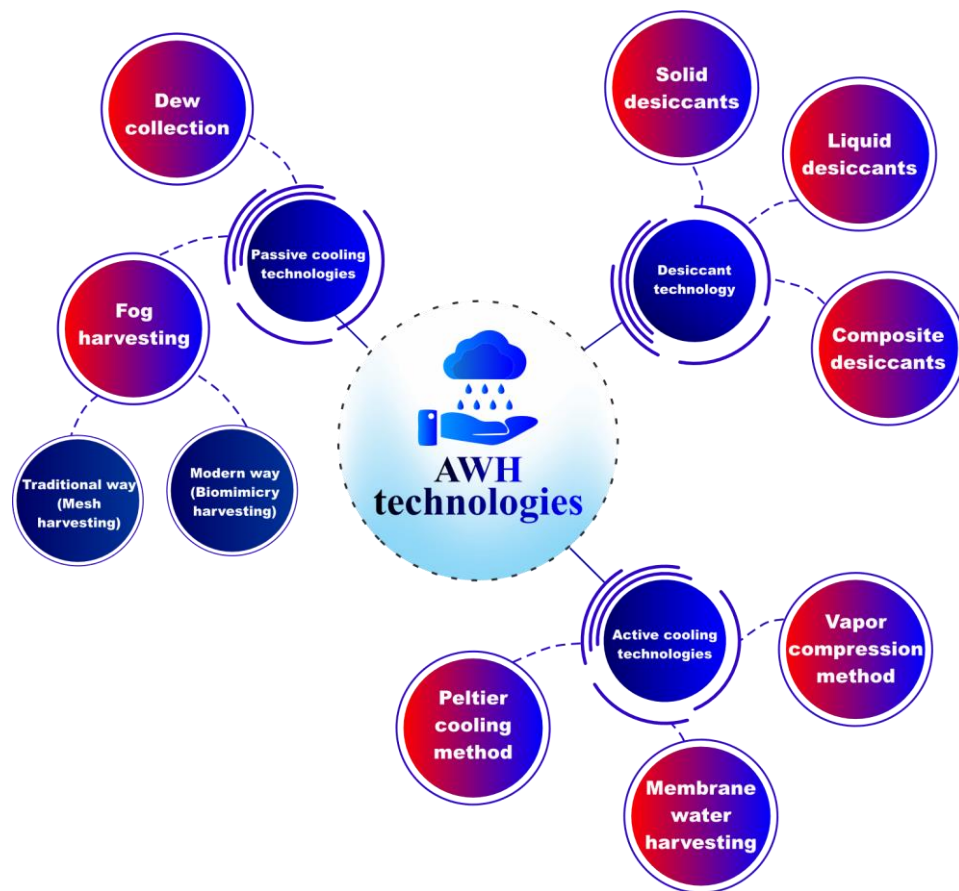


Fig. 1. Classification of AWH technologies summed up in active, passive, and desiccant cooling categories.

1150

Year	Patent #	Title	Title	Patent #	Year
1900	US 661944	Apparatus for removing moisture from air	Apparatus and method for harvesting atmospheric moisture	US 6945063B2	2004
1938	US 2138689	Method for gaining water out of the atmosphere	Apparatus and method for extracting potable water from atmosphere	US 6755037B2	2004
1946	US 2409624	Apparatus for extracting water from atmospheric air	Water from air using liquid desiccant and vehicle exhaust	US 200701018262A1	2005
1956	US 2761292	Device for obtaining fresh drinkable water	Production of drinking water from air	US 6960243	2005
1957	US 2805560	Method and apparatus for condensing moisture	Device for the extraction of water from atmospheric air	US 7722706B2	2006
1970	US 3498077	Atmospheric water recovery method and means	Device for collecting water from air	US 7043934	2006
1973	US 3777456	Extracting water from the atmosphere	Apparatus and methods for creating sparkling water from atmosphere	US 7861544B2	2011
1979	US 4146372	Process and system for recovering water from the atmosphere	Composite desiccant and air-to-water system and method	US 8506675B2	2013
1981	US 4255937	Atmospheric water collector	Water Adsorption device	US 2014/352536A1	2014
1984	US 4433552	Apparatus and method for recovering atmospheric moisture	Atmospheric water harvesters	US 8627673B2	2014
1992	US 5106512	Portable air-water generator	Water recovery system and method	US 8834614B2	2014
1993	US 5233843	Atmospheric moisture collection device	Extraction of water from air	US 9200434B2	2015
1996	US 5553459A	Water recovery device for reclaiming and refiltering atmospheric water	Systems and methods for generating liquid water from air	US 0354920A1	2017
1999	US 5857344	Atmospheric water extractor and method	Sorption-based atmospheric water harvesting device	US 2018/0171604A1	2018
2001	US 6230503B1	Method and apparatus for extracting water from air	Systems and methods for water extraction control	US 2018/0043295A1	2018
2002	US 6336957B1	Method and apparatus for extracting water from atmospheric air	Hybrid atmospheric water generator	US 2018/0209123A1	2018
2002	US 20020189448A1	Method and apparatus for extracting water from air using a desiccant	Materials for moisture removal and water harvesting from air	US 10486102B2	2019

1151

1152

Fig. 2. Comprehensive detail of AWH patents published in the literature

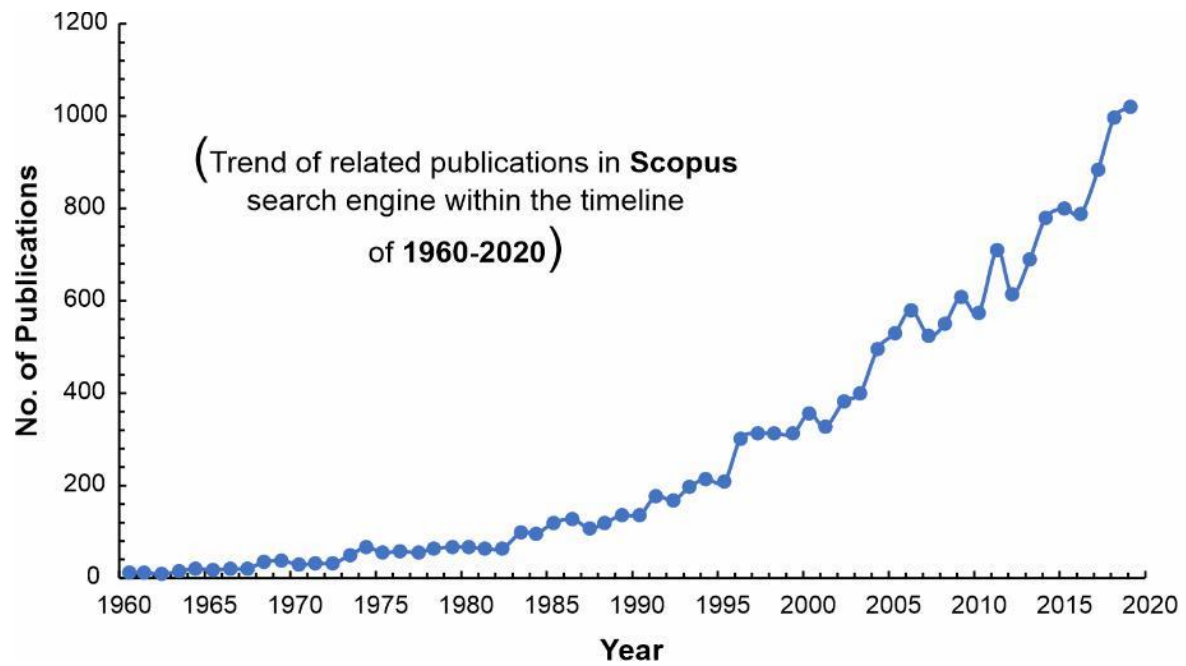


Fig. 3. No. Publications in the field of AWH in Scopus search engine from 1960-2020.

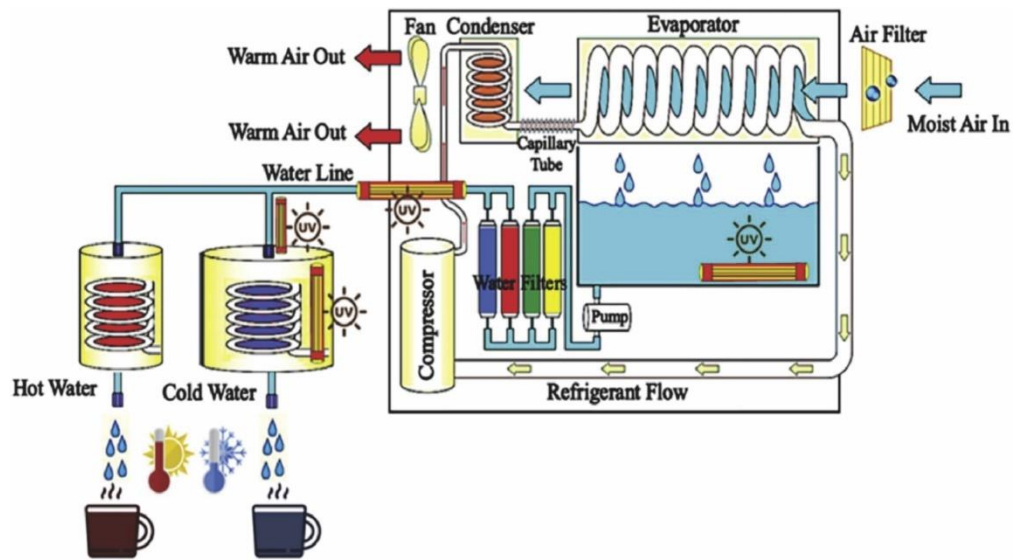


Fig. 4. (a) Schematic of AWH system based on VCC process [162].

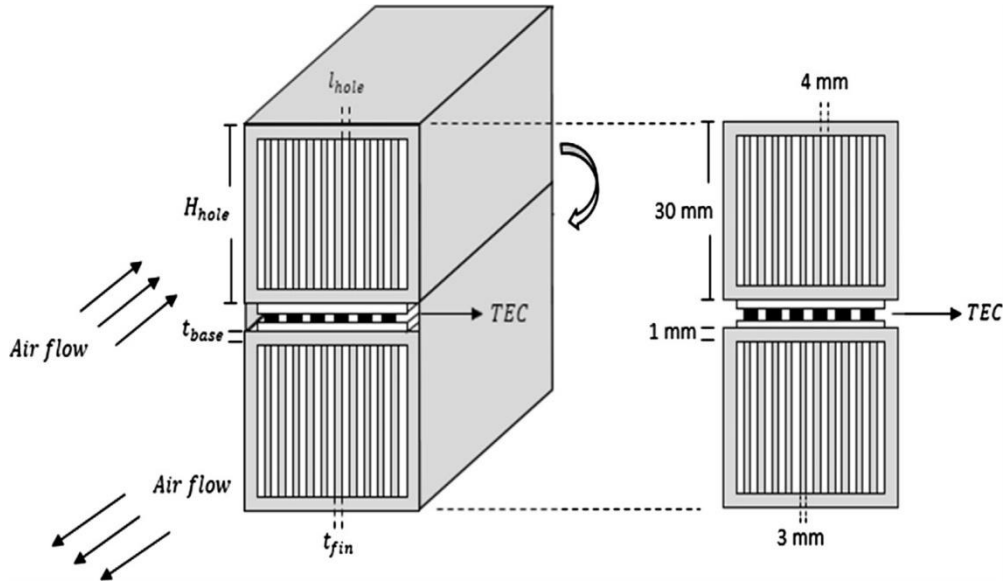


Fig. 5. Schematic of the TEC system installed for water production [40].

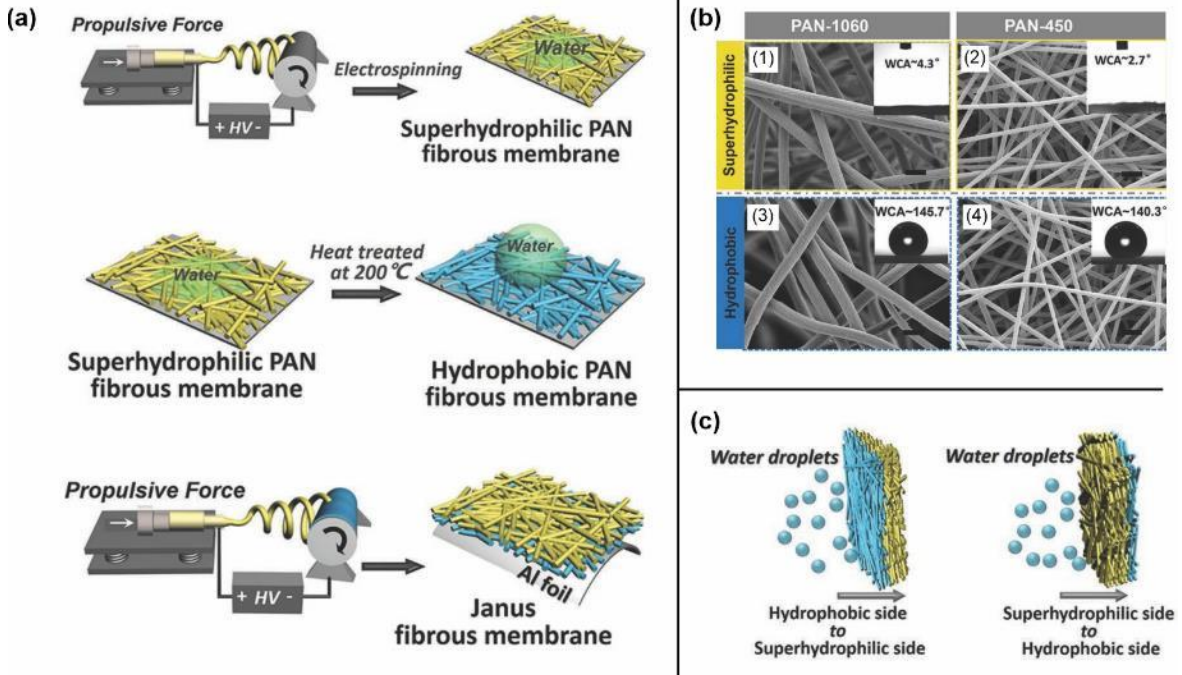


Fig. 6. (a) Process of the fibrous membrane fabrication for AWH (b) SEM images of PAN-1060 and PAN 450 fibrous membranes before and after heat treatment (c) Illustration of water harvesting mechanism by membranes [45].

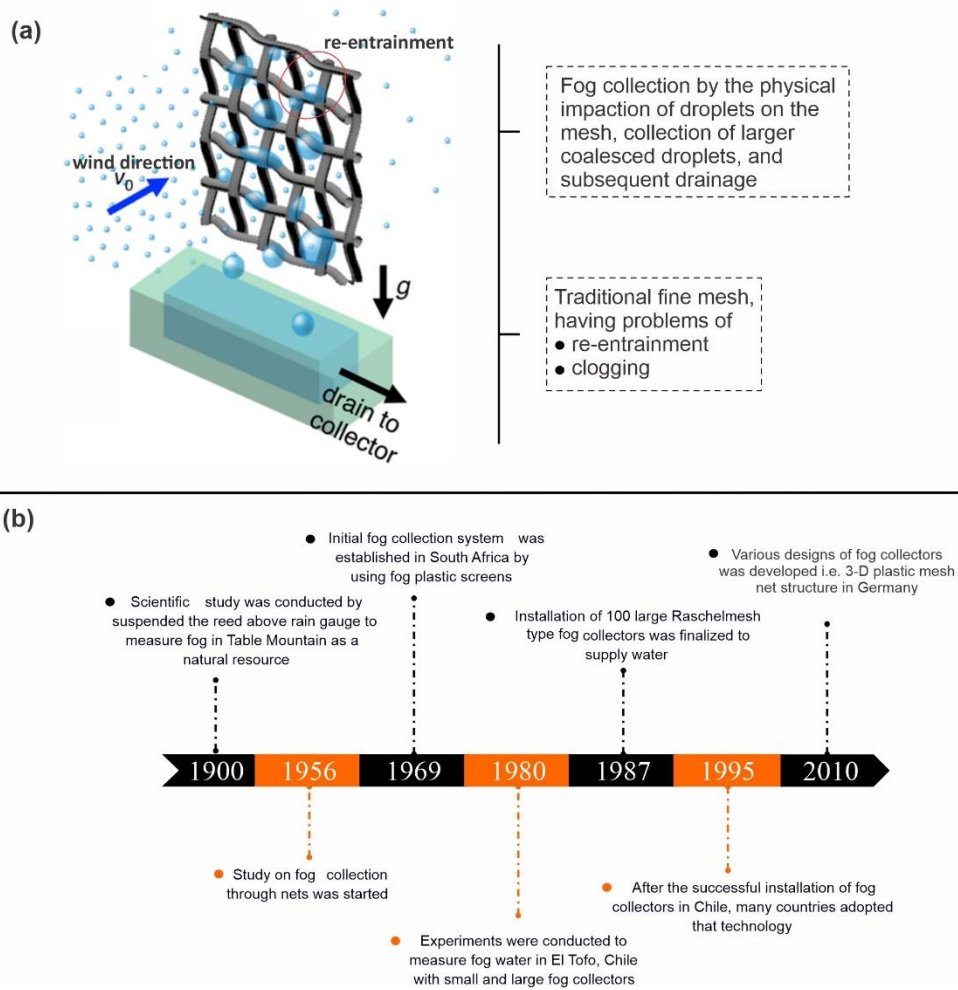


Fig. 7. Fog water harvesting (a) mechanism of fog collection on the mesh [54] (b) progress of major developments in fog water collection technology [163].

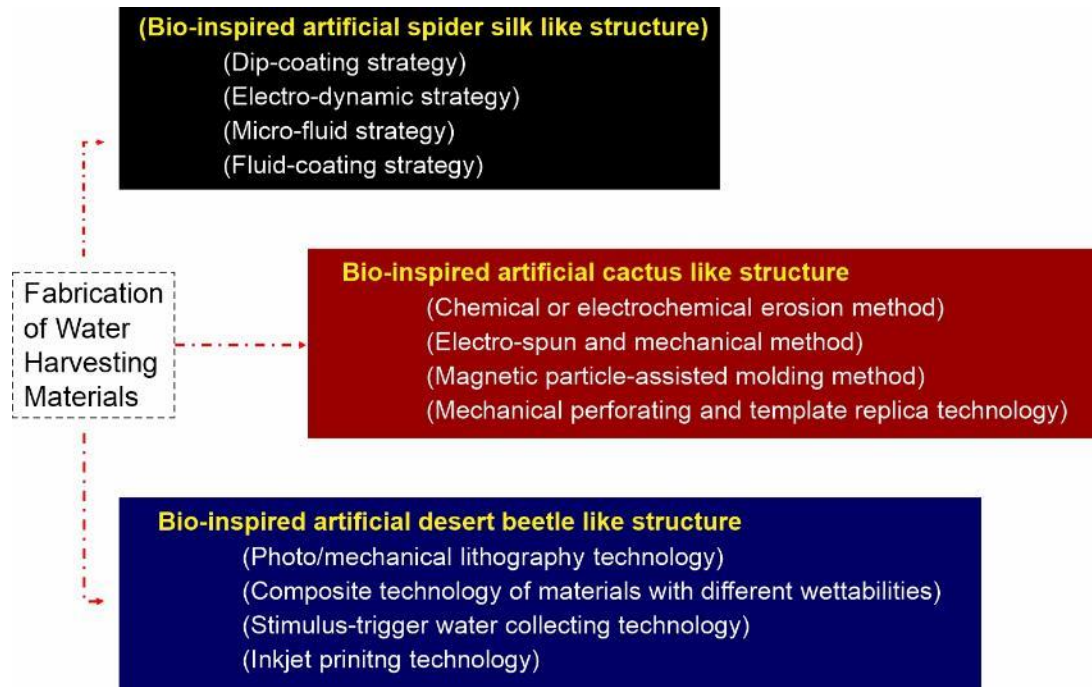


Fig. 8. Technologies for the fabrication of bio-inspired water harvesting materials [164].

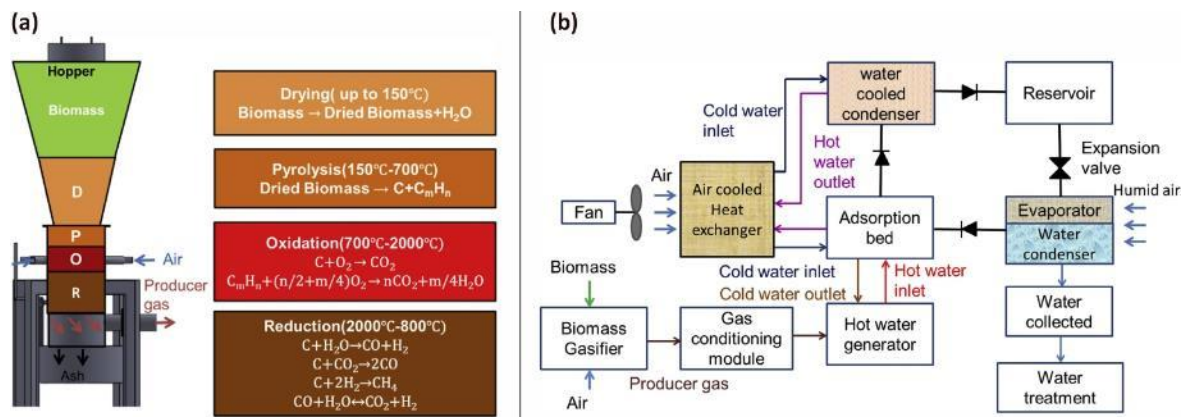


Fig. 9. Biomass gasification based AWH system (a) schematic of a downdraft gasifier used in AWH system (b) presentation of biomass gasification based system for AWH [60].

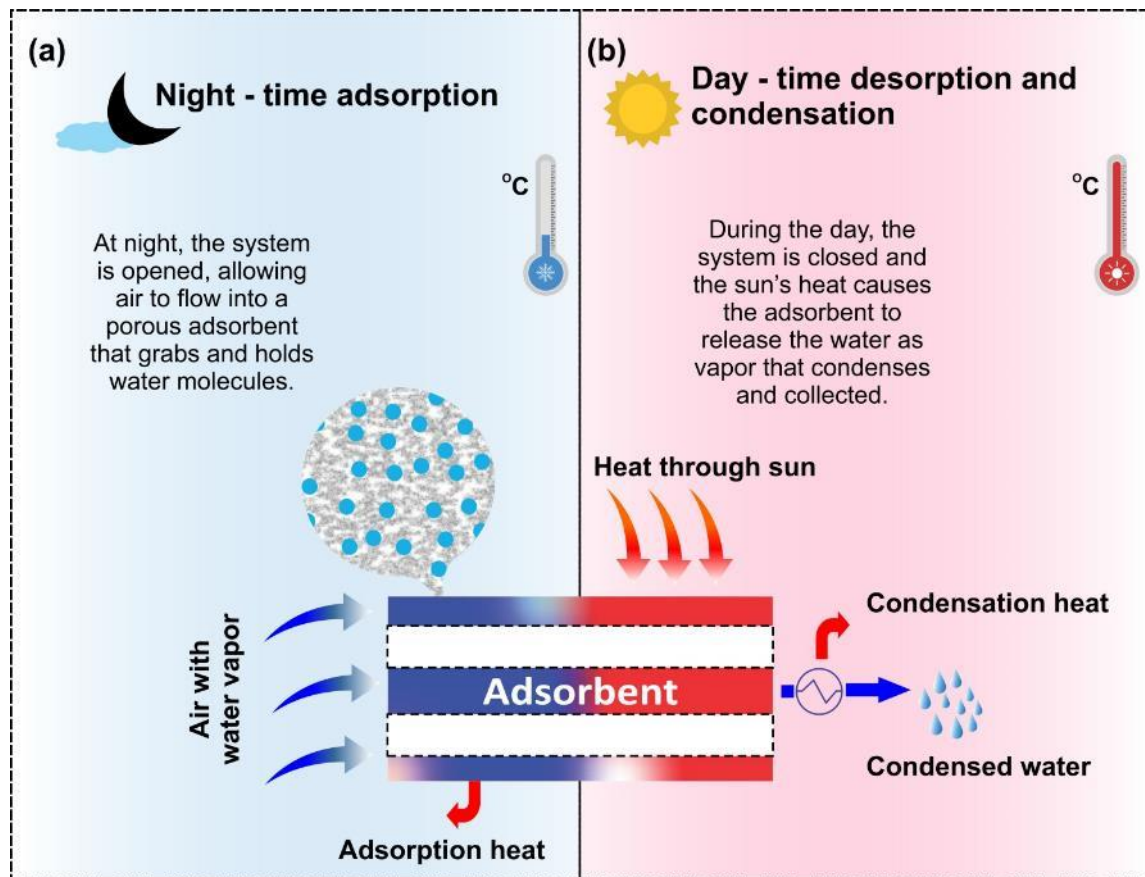


Fig. 10. Illustration of the principle of adsorption based AWH showing adsorption phase during night-time and desorption and condensation phase during the daytime.

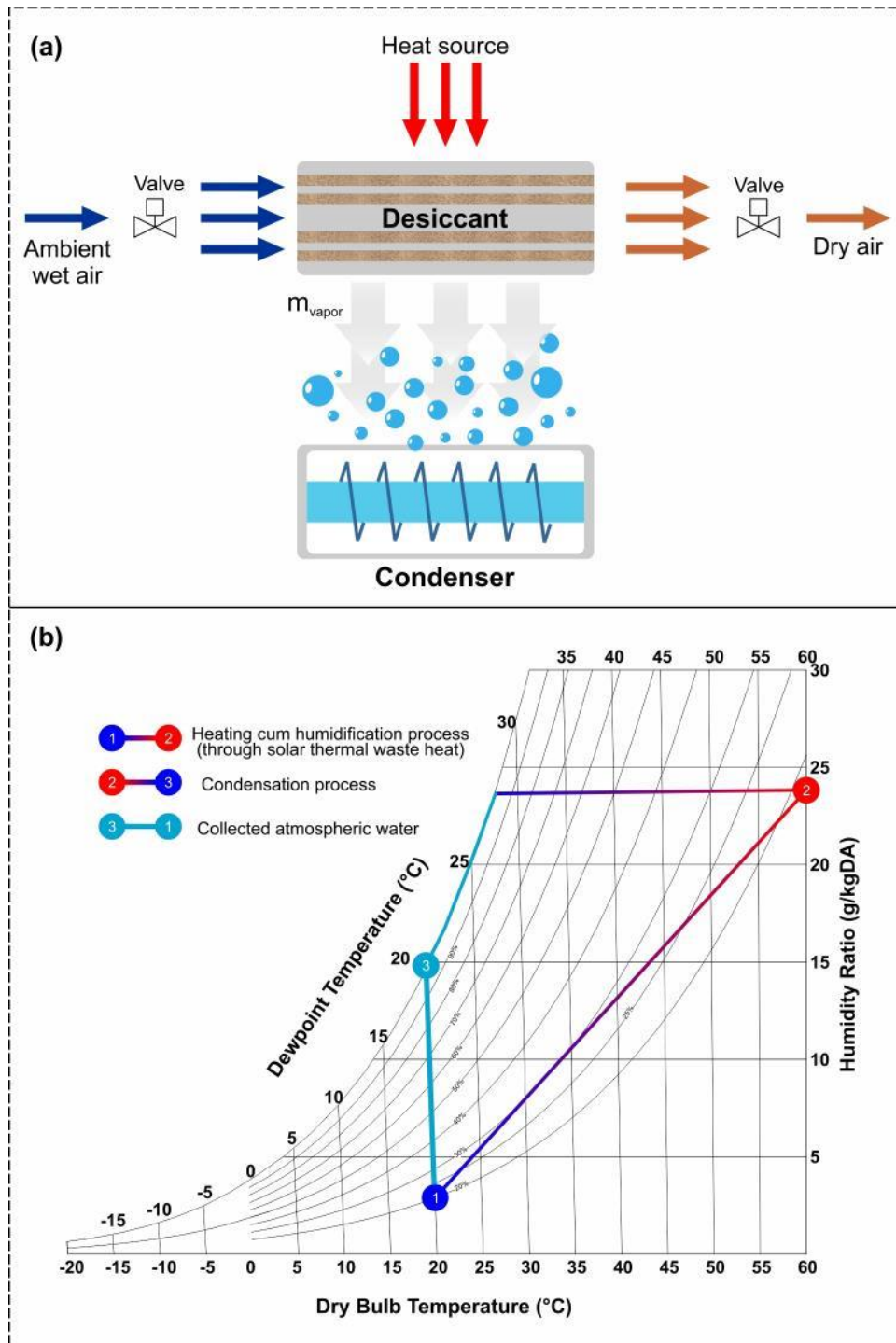


Fig. 11. Representation of a typical adsorption-based AWH system (a) schematic comprises of adsorbent material and a condenser (b) psychrometric representation showing humidification, condensation, and collection processes of atmospheric water.

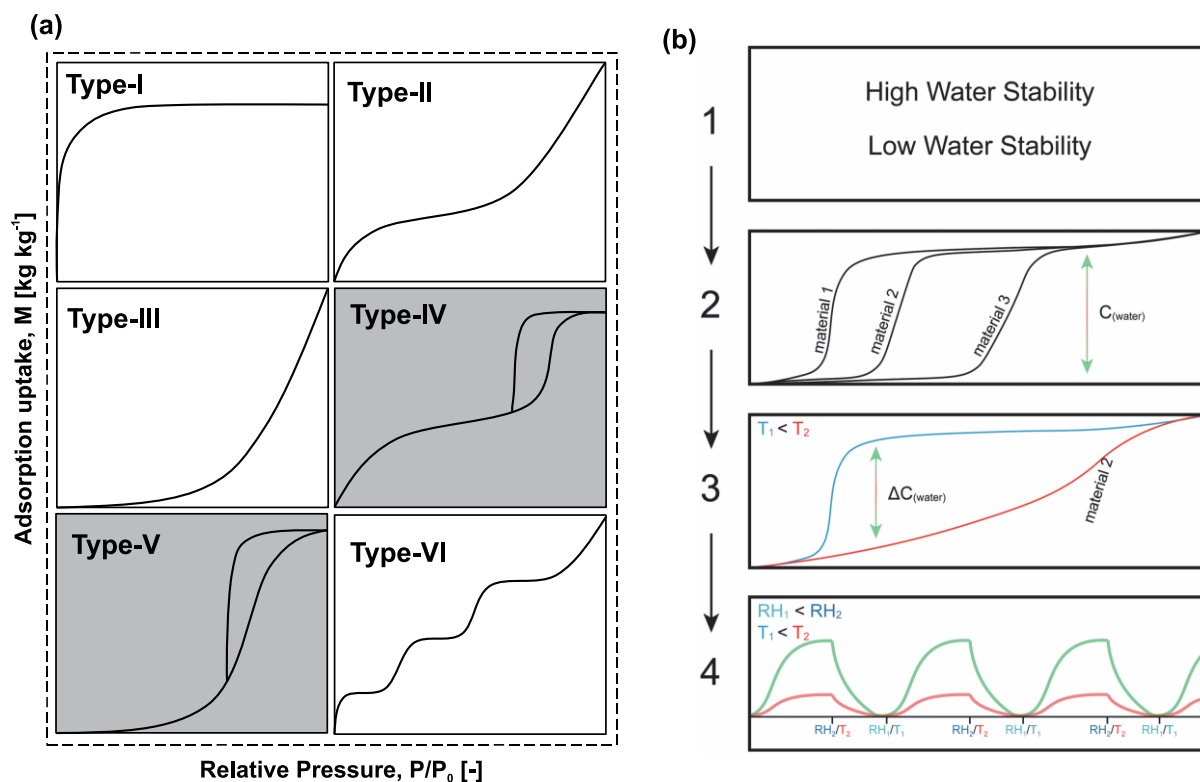


Fig. 12. (a) Classification of adsorption isotherms from type-I to type-VI, also, desired isotherms (type-IV and type-V) for AWH are highlighted [91,165] (b) Presentation of the selection criteria (high stability of water, suitable isotherm, efficient adsorption at variant temperatures, and kinetics of materials) for suitable MOFs used in AWH [15].

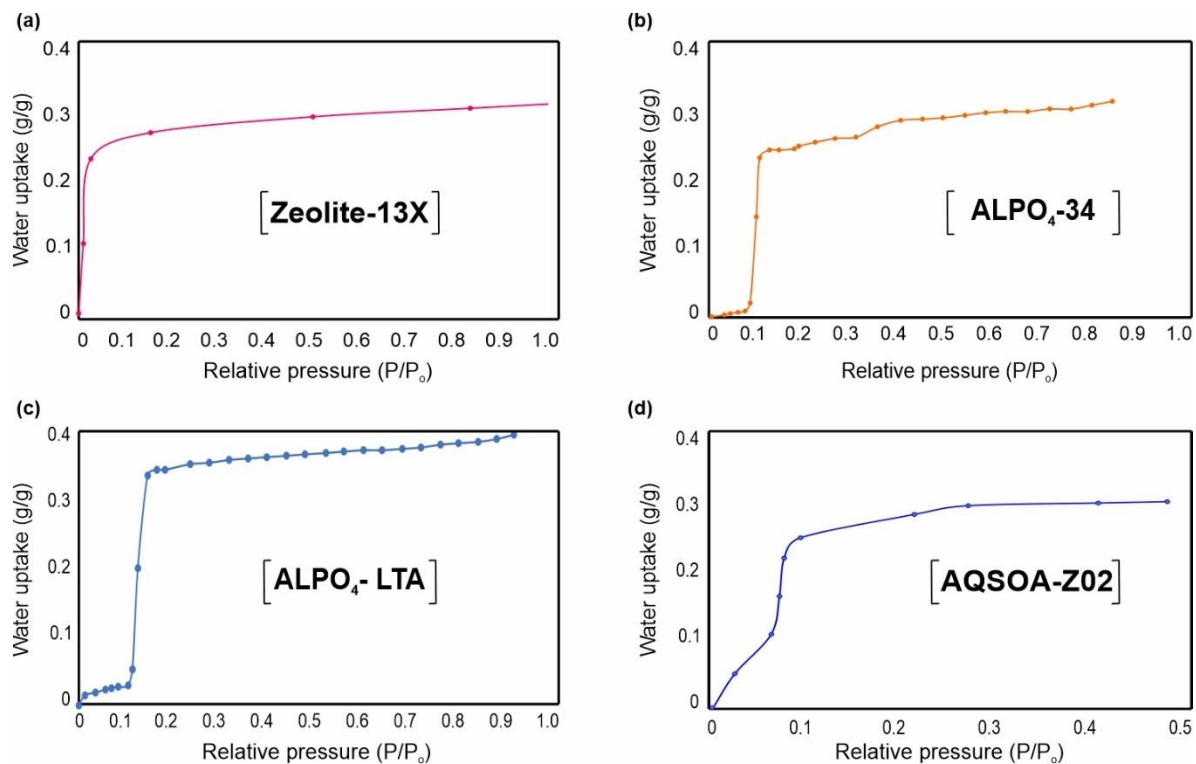


Fig. 13. Graphical representation of water adsorption isotherms of microporous aluminophosphate zeolites for AWH extracted from the literature: (a) Zeolite-13X [17], (b) ALPO₄-34 [135], (c) ALPO₄-LTA [135], and (d) AQSOA-Z02 [166].

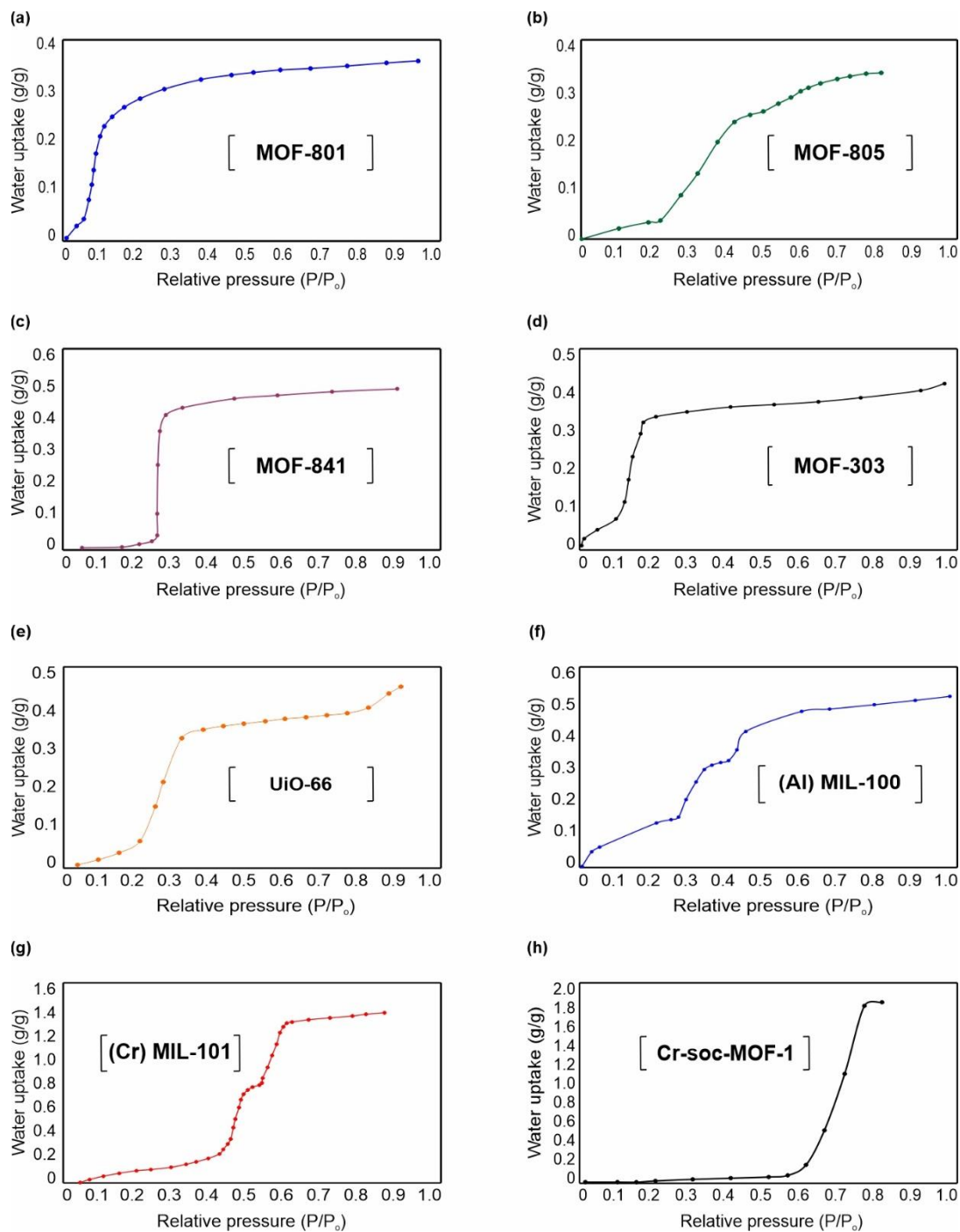


Fig. 14. Graphical representation of the water adsorption isotherms of suitable MOFs for AWH extracted from the literature: (a) MOF-801 [67], (b) MOF-805 [137], (c) MOF-841 [137], (d) MOF-303 [69], (e) UiO-66 [17], (f) Al-MIL-100 [167] (g) Cr-MIL-101 [168], (h) Cr-soc-MOF-1 [169].

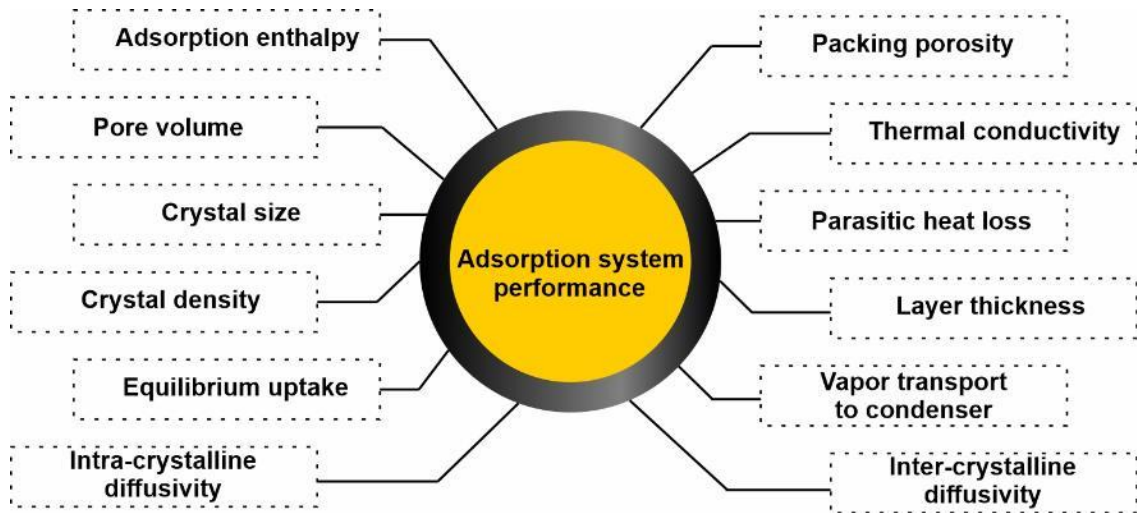


Fig. 15. Illustration of the material and component level properties dictated the adsorption-based AWH system performance reproduced from [51].

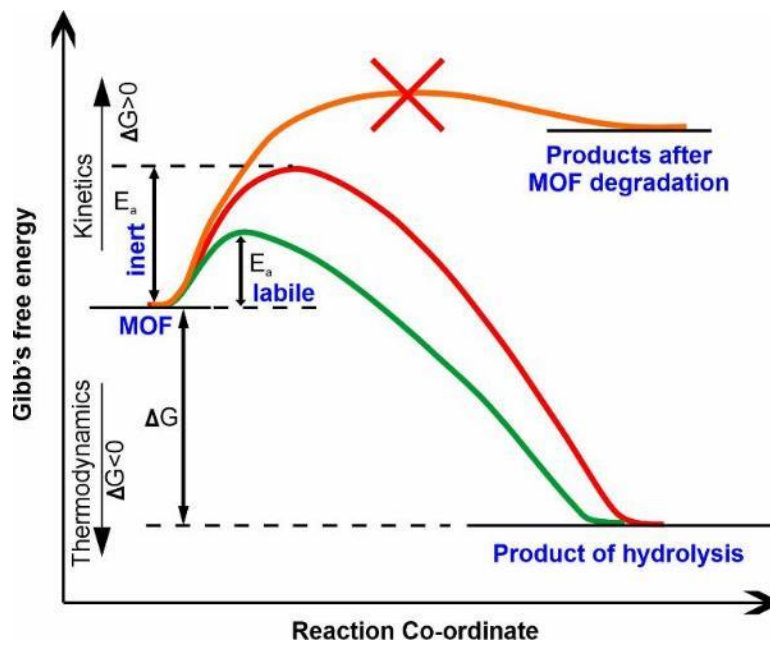


Fig. 16. Reaction coordinate diagram illustrating the effect of degradation of MOFs with thermodynamic and kinetic stability. Cross symbol indicating the route's unfeasibility [15].

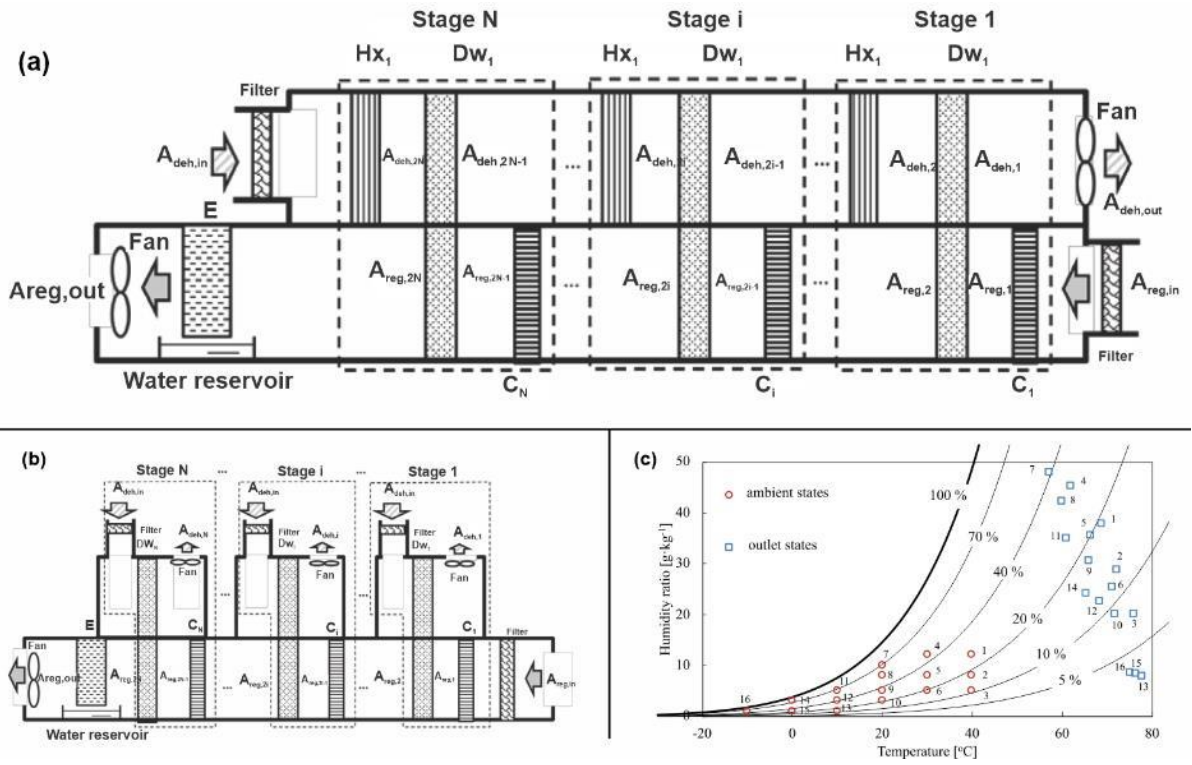


Fig. 17. AWH from multi-stage desiccant wheel systems (a) and (b) schematics of two scenarios for desiccant wheel heat pump based AWH system (c) representation of studied ambient/inlet and outlet conditions [131].

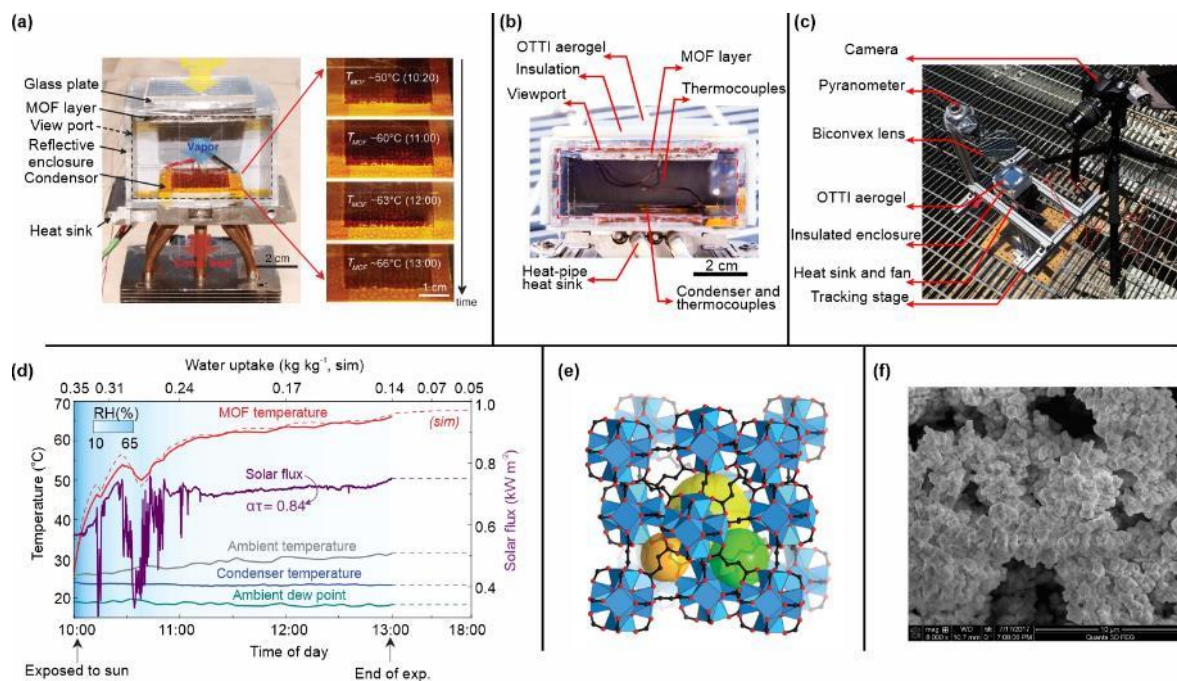
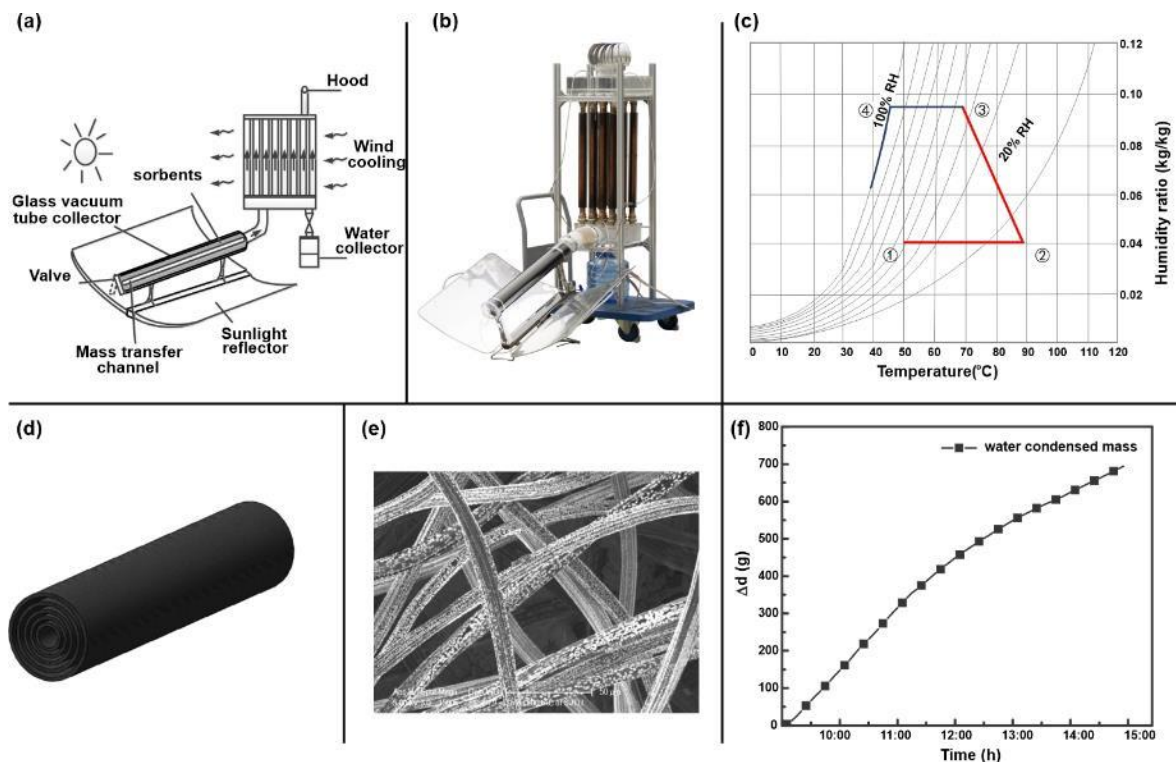


Fig. 18. Proof of concept MOF-801 based AWH system (a) pictorial representation of MOF-801 based AWH prototype. (b) image of the AWH apparatus exposing the MOF-layer (c) AWH device test apparatus at AZ, USA. (d) representation of MOF temperature, solar flux, ambient air temperature, condenser, and ambient dew point temperature profiles (e) crystal structure of MOF-801, and (f) SEM image of MOF-801 [61,67].

1240



1241

1242 **Fig. 19.** Small concept ACF-CaCl₂ based AWH machine. (a) schematic of AWH machine (b) pictorial
1243 representation of the test apparatus (c) psychrometric representation of AWH phenomenon (d) structure of ACF-
1244 CaCl₂ material used in AWH machine (e) SEM image of ACF matrix with CaCl₂. (f) graphical representation of
1245 the water condensation rate [62].

1246

1247

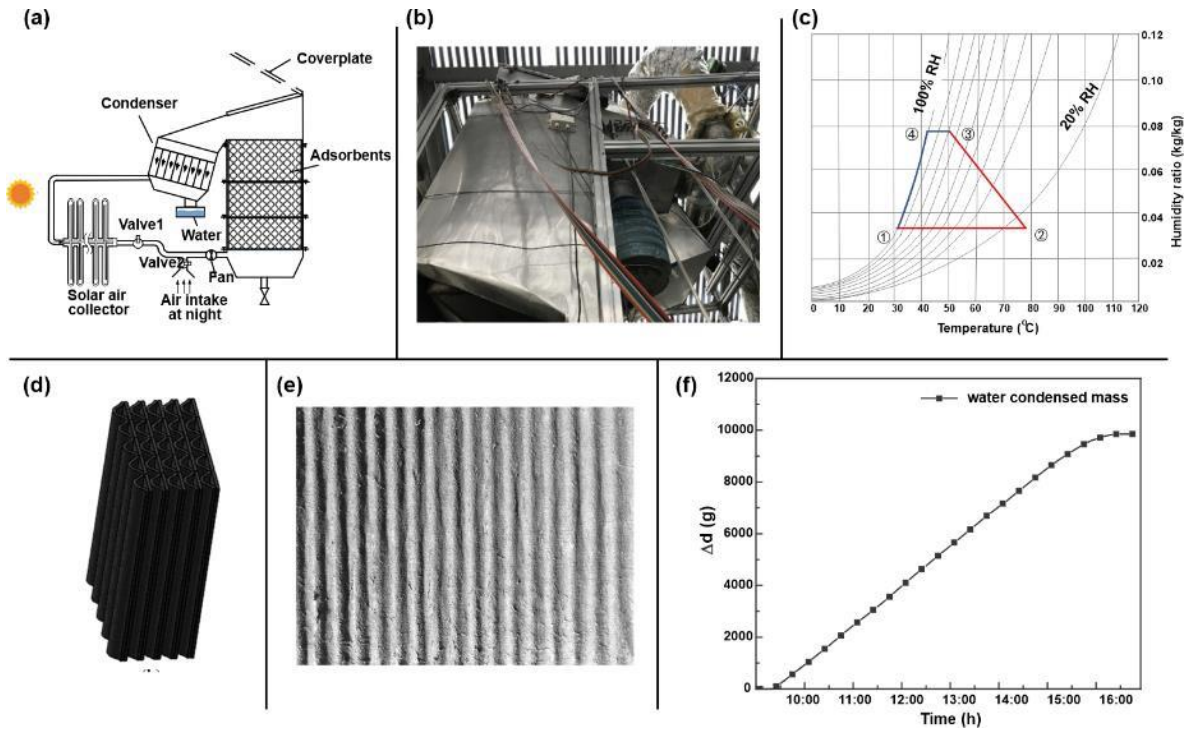


Fig. 20. Semi-open solar-driven ACF-LiCl-based AWH device. (a) schematic of AWH system (b) pictorial representation of the real test unit (c) psychrometric representation of AWH phenomenon (d) ACF-LiCl material used in AWH device (e) SEM image of consolidated composite with LiCl sorbent (f) graphical representation of the water condensation rate [62].

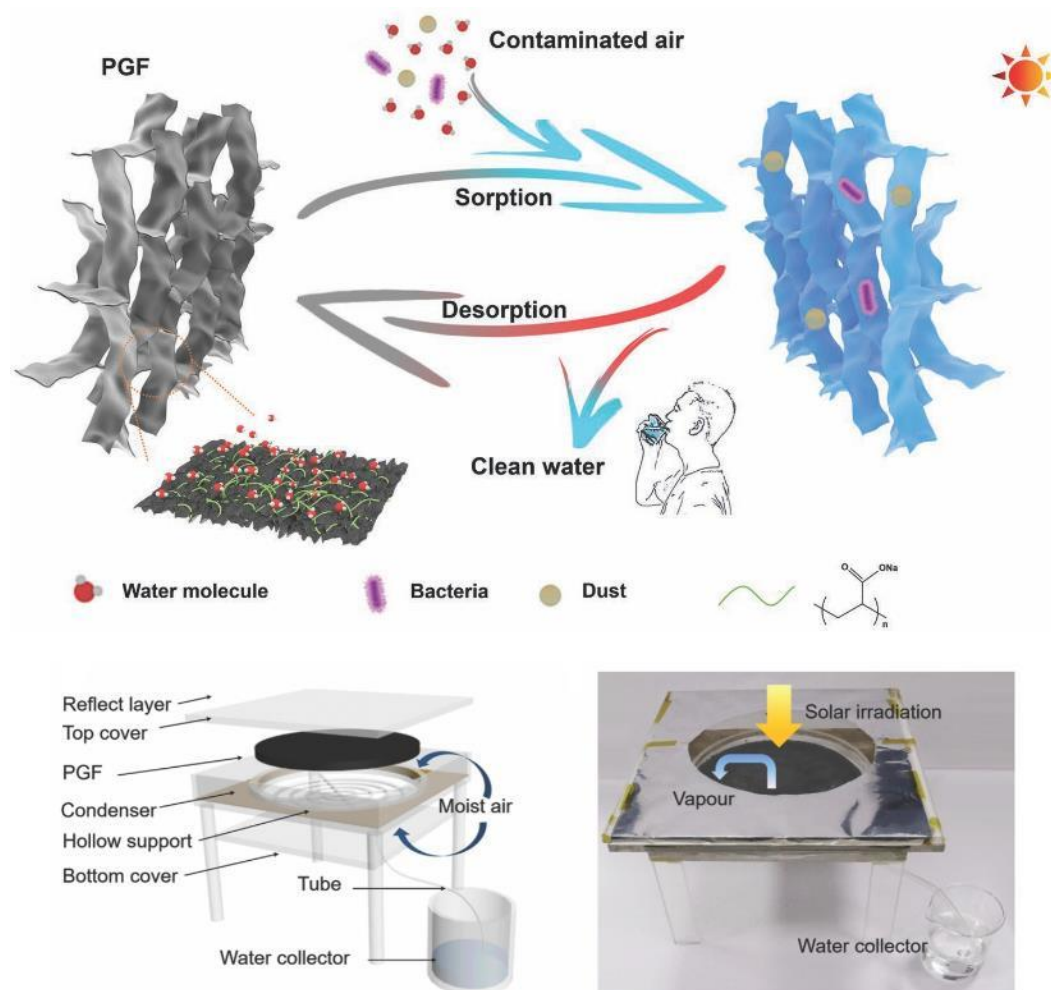


Fig. 21. Illustration of sodium polyacrylate/graphene framework for AWH from the contaminated air [146].

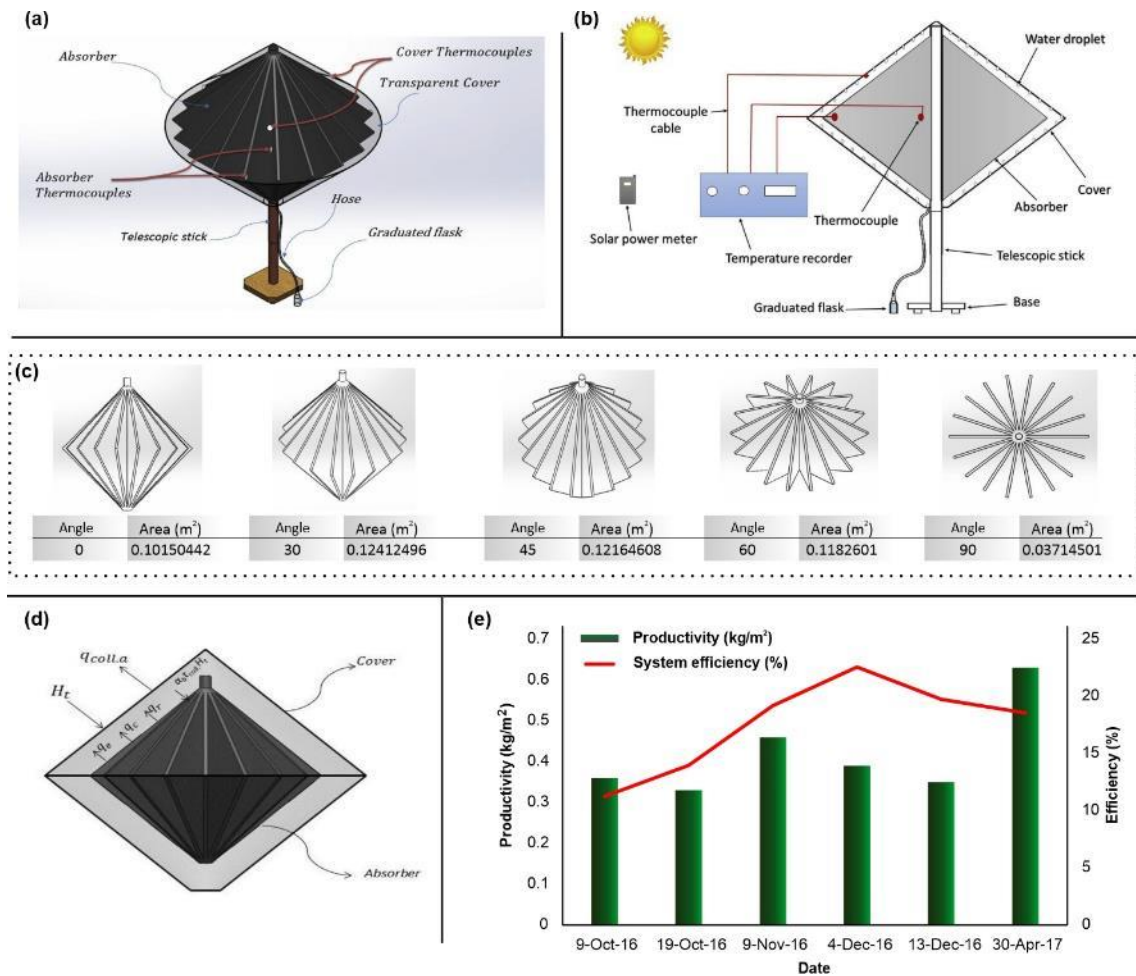


Fig. 22. Calcium chloride desiccant based AWH system (a) illustration of the experimental unit (b) sectional view of the test apparatus (c) area of an absorber of the experimental system at different altitude angles (d) energy flow diagram of an experimental system (e) graphical representation of the water production rate with system efficiency [153].

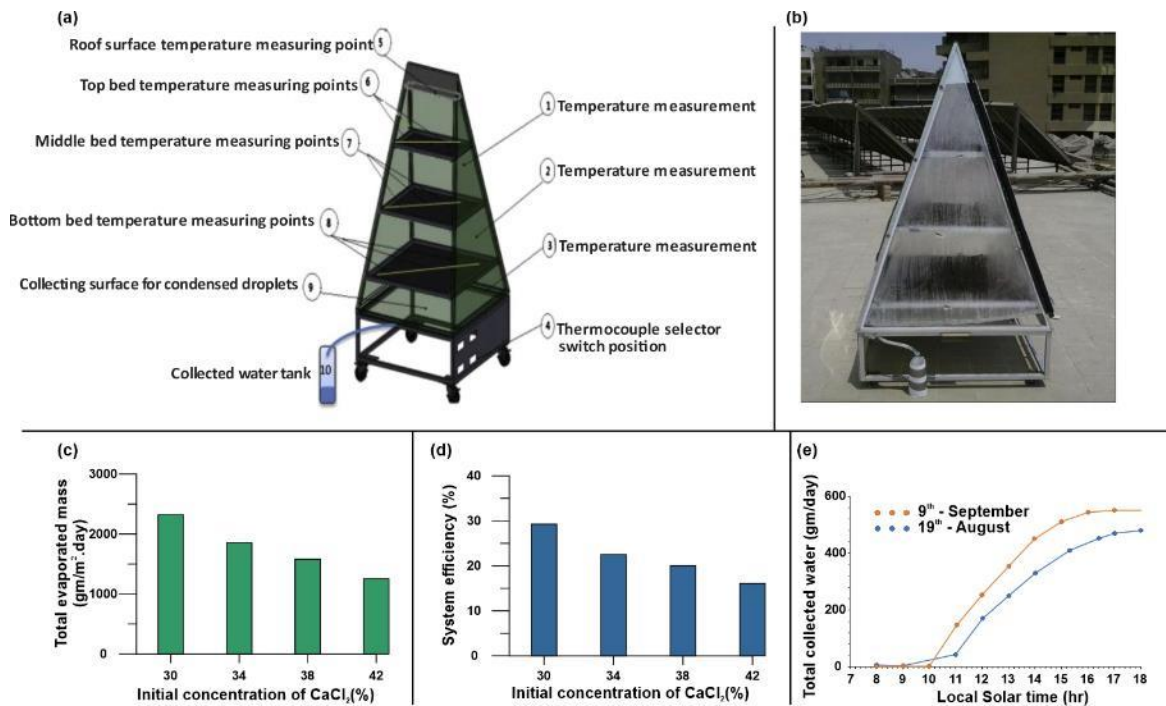


Fig. 23. Calcium chloride desiccant based solar AWH system (a) illustration of the schematic diagram of an experimental setup (b) physical representation of the test apparatus (c) variation of total evaporated mass in the system (d) graphical representation of the system efficiency for cloth bed (e) representation of the water collection rate for cloth bed [154].

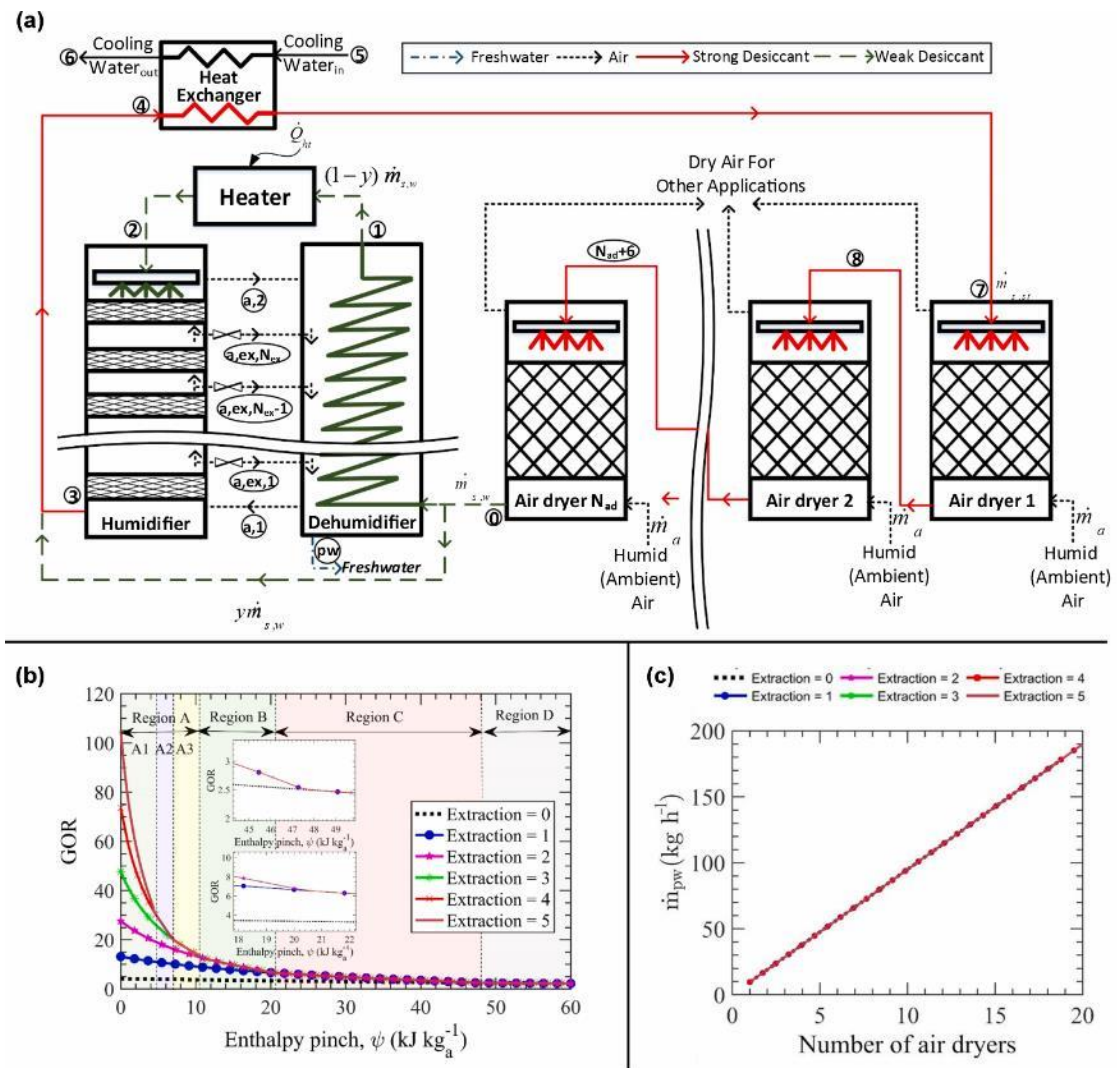


Fig. 24. (a) Liquid desiccant-based humidification-dehumidification AWH system (b) representation of relation between enthalpy pinch and GOR for various extractions (c) effects of the number of dryers on the WHR of system [170].

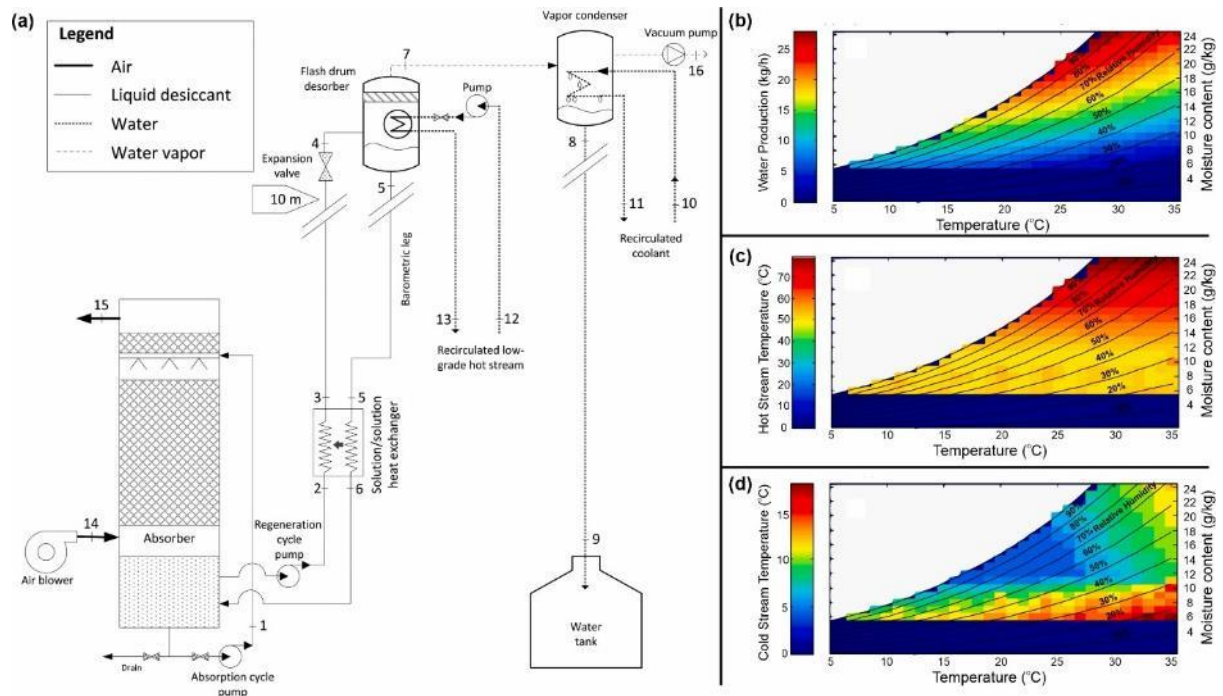


Fig. 25. (a) Liquid desiccant-based vapor separation AWH system (b) representation of the water production rate under ambient conditions (c) and (d) hot and cold stream temperature results for desorber and the condenser under ambient conditions [160].

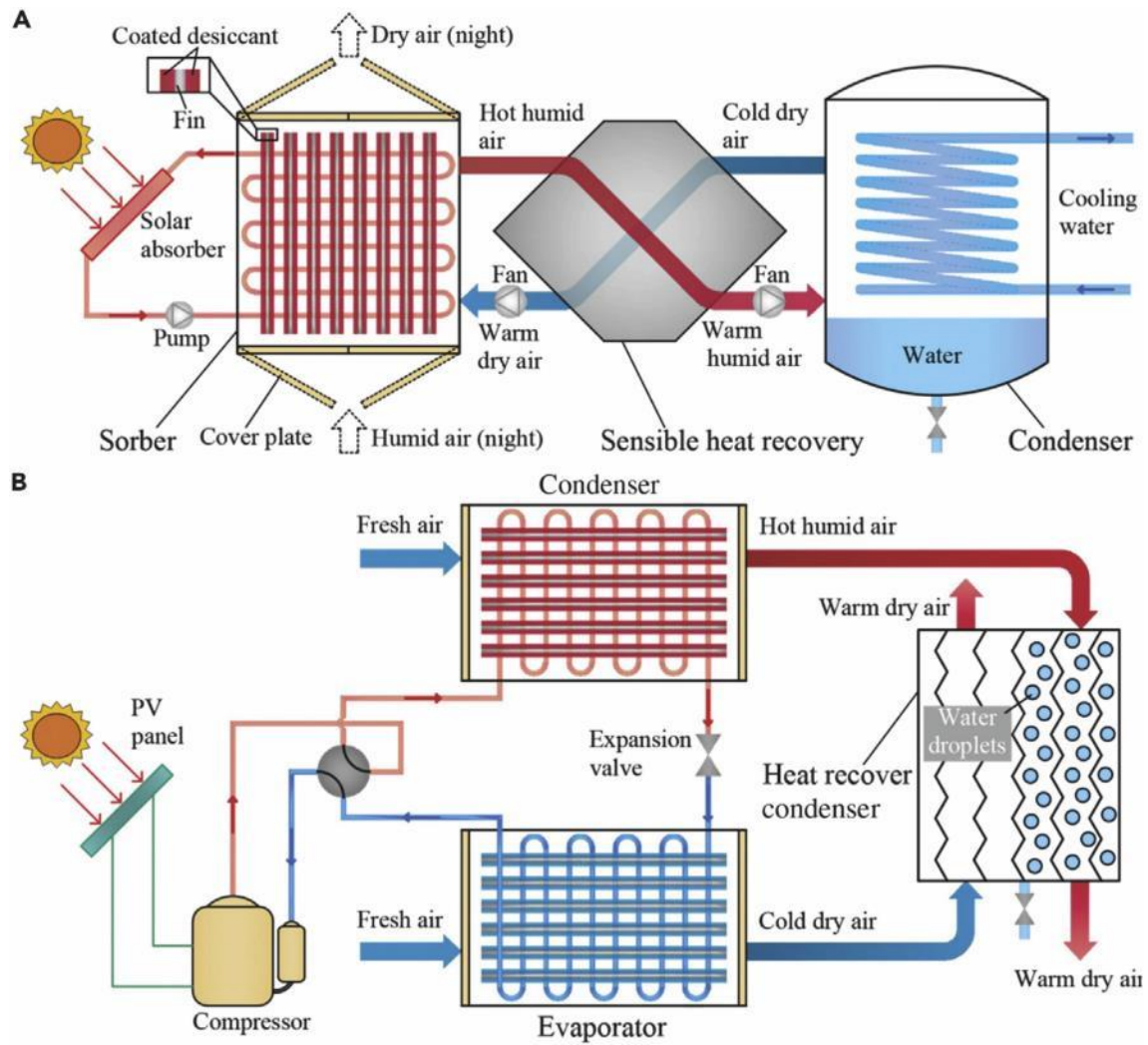


Fig. 26. (a) Illustration of the solar water heating driven atmospheric water generator (b) representation of solar PV powered atmospheric water generator with desiccant heat pump (optimal for those regions where continuous water production is required) [17].

1291 **List of Tables**

1292

1293 **Table 1.** Summary of the selected VCC and TEC systems for AWH [47].

Method	System Information	Ambient Conditions	WHR (kg h ⁻¹)	UPC (kWh kg ⁻¹)	Ref
VCC					
VCC	Frontal area = 0.04 m ²	-	0.92 - 1.08	0.22 - 0.3	[30]
VCC	Refrigerant = R22 Compressor power = 370W Cooling capacity = 1.5 kW	35°C, 20% - 40% RH	0.13 - 2	2.8 - 0.18	[171]
VCC	Airflow rate = 578 m ³ h ⁻¹ Compressor power = 1035W.	DBT = 26.7° C, WBT = 19.4° C	1.5	0.69	[29]
TEC					
TEC	TECs = 18 in series	35° C, 70% - 100% RH	20×10 ⁻³ – 106×10 ⁻³	2.5 – 1.22	[40]
TEC	Photovoltaic power = 145 W	-	2×10 ⁻³ – 4×10 ⁻³	-	[172]
TEC	Weight = 7 kg Cold side fins area = 0.216 m ²	23.1° C – 24.5° C, 65% - 95% RH	11.2×10 ⁻³ - 25.1×10 ⁻³	5.21 - 2.33	[173]

1294

Table 2. Features of the selected animals and plants studied for AWH.

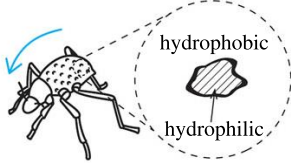
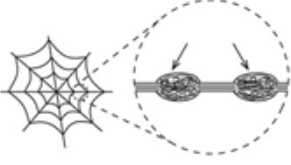
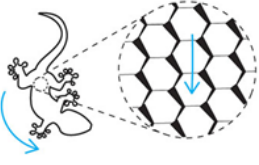
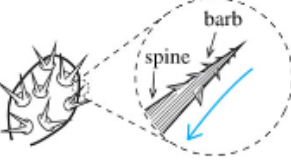
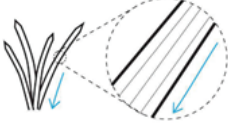
Animals/Plants	Species	Mechanism	Information learned	Ref.
Insects (Beetles)	Stenocara sp.	 [174]	Heterogeneous wettability	[175]
Spider	Uloborus walckenaerius	 [174]	Laplace pressure gradient	[55]
Reptiles (lizards)	Moloch horridus	 [174]	Grooves	[176,177]
Cactus	Opuntia microdasys	 [174]	Grooves	[178]
Grass	Stipagrostis sabulicola	 Channelling via grooves [174]	Grooves	[179]

Table 3. Compilation of some of the potential adsorbent materials for AWH.

MOFs and Zeolites used in AWH systems								
Material	Gravimetric uptake (g/g)	Regeneration temperature (°C)	Adsorption condition			Adsorption enthalpy (KJ/L)	Harvesting capacity (g/g)	Ref
			T (°C)	RH (%)	Vapor pressure (mbar)			
MOF-801	0.38	85	25	70	22.2	3050	0.25	[61,67]
Co-BTDD	0.87	55	25	70	22.2	3050	0.72	[96]
Cr-soc-MOF-1	2	-	25	70	22.2	-	-	[169]
Al-Fumarate	0.34	65	-	-	-	2780	0.33	[15,97]
AQSOA Z02	0.3	95	-	-	-	3420	0.23	[94,166]
AlPO ₄ -LTA	0.38	75	-	-	-	3050	0.37	[135]
AlPO ₄ -34	0.29	75	-	-	-	3220	0.28	[135]
Hygroscopic and Inorganic/Organic materials used in AWH systems								
Material	Host materials	System	Relative humidity (%)	Quantity of material	Harvesting capacity	Ref		
CaCl ₂	Silica gel	Solar driven	50-80	10 kg	3-5 L	[180]		
CaCl ₂	Cloth	Tilted glass flat plate solar collector	24-76	-	1.5 L/m ² per day	[148]		
CaCl ₂	SiO ₂	Glass cylindrical absorber	50-100	10 kg	5 L	[26]		
CaCl ₂	MCM-41	Solar driven	78-92	1 kg	1.5 L	[142]		
CaCl ₂	Sand	Solar driven still	40	1 kg	1 L/m ² per day	[155]		
CaCl ₂	Wick	Solar driven still	50	3.7 kg	1.4 L/m ² per day	[181]		
CaCl ₂	Activated carbon	-	30	-	0.23 g/g	[182]		
CaCl ₂	Alginate-derived hydrogel matrix	-	26	-	660 kg/m ³ of bulk material	[64]		
LiCl	Sand	Scheffler reflector solar thermal system	36-68	1.5 kg	0.115 L/day	[183]		
LiCl	Active carbon felt	Semi open system	85	40.8 kg	14.7 L	[66,184]		
LiCl	Nanocarbon hollow capsule	Metallic cookie box	15-80	-	1.6 g/g	[185]		
CuCl ₂	Silica fibrous filter	Bilayer water collection device	15-60	1 kg	0.35 L	[186]		

LiBr	Porous carbon	-	70	-	0.6-1.1 ml/g	[187]
Super hygroscopic hydrogel	-	Box type system	80-90	1 kg	10 L/day	[188]

1299

1300

Table 4. Summary of the selected MOFs with high adsorption properties and performances.

Material	Linker	Topology pore structure	Stability	Pore size(Å)	α	$d_{\text{cryst}}(\text{g cm}^{-3})$	$q_{\text{max}}(\text{g g}^{-1})$	$V_p(\text{cm}^3\text{g}^{-1})$	Ref
Cr-soc-MOF-1	TCPT	-	Over 100 adsorption cycles, no loss in Δq is reported	-	0.69	-	1.95	2.1	[169]
MIL-101(Cr)	BDC	mtn,3D	-	29,34	0.46	0.61	1.73	1.68	[168,189],[93]
CO ₂ Cl ₂ (BTDD)	BTDD	-	Over 30 adsorption cycles, 6.3% loss in Δq is reported	-	0.29	-	0.97	-	[96]
MOF-841(Zr)	MTB	flu,3D	-	9.2	0.22	1.05	0.51	0.53	[137]
Y-shp-MOF-5	BTEB	shp,1D	After 1000 adsorption cycles, 9% loss in q_{max} with significant hysteresis is reported	12	0.63	0.97	0.48	0.63	[190]
MOF-303(Al)	PDC	-	Over 5 adsorption cycles, no loss in q_{max} is reported	-	0.13	-	0.45	0.54	[69]
MOF-801(Zr)	FA	fcu,3D	Over 5 adsorption cycles, material is stable	4.8,5.6,7.4	0.09	1.68	0.36	0.45	[137]
UiO-67	BPDC	fcu,3D		8.8,16.6	0.56	1.04	0.3	0.99	[191]
MIL-53(Al)	BDC	sra,1D	-	7-13	0.75	-	0.40	0.51	[192],[93]
MIL-160(Al)	FDC, furan	yfm,1D	Over 10 adsorption cycles, no loss in Δq is reported	5	0.09	-	0.38	0.40	[193]
CAU-10(Al)-H	1,3-BDC		Over 9 adsorption cycles, no loss in Δq is reported	7	0.16	1.37	0.37	0.43	[194],[195]
UiO-66(Zr)	BDC	fcu,3D	Over 2 adsorption cycles, no	7.4	0.31	1.23	0.37	0.35	[196],[197],[137]

			loss in q_{\max} is reported						
Al-fumarate	FA	-	Over 4500 adsorption cycles, no loss in Δq is reported	-	0.27	-	0.45	0.48	[198]
MIP-200(Zr)	MDIP	-	Over 1-10 adsorption cycles, 6% loss Δq is reported, and over 10-40 adsorption cycles, no loss in Δq is reported,	-	0.18	-	0.45	0.40	[199]

1302

1303

1304 **Table 5.** Thermal conductivity of different adsorbents with different measurement techniques in the literature.

Material	Thermal conductivity (Wm ⁻¹ k ⁻¹)	Temperature (° C)	Measurement method	References
Silica gel	0.147	21.85	Transient hot strip	[200]
Silica gel material with CaCl ₂ and graphite	0.41	34.85	-	[201]
Composite silica gel KSK with CaCl ₂	0.112	19.85	Transient hot wire	[202]
Graphite with silica gel	3.7-19.1	-	-	[124]
Graphite with metal chloride	10-40	-	-	[121]
SAPO-34 CHA + Al	9			[203]
AQSOA FAM-Z01	0.376	19.85	Laser flash	[204]
Activated Carbon	0.5	-	-	[205]
Monolithic carbon	0.35-0.44	-	-	[206]
MOF-5	0.32	26.85	Heat flow method	[207]

1305

1306
1307

Table 6. Comparison among the various methods for AWH reported in the literature [162].

Comparison	Fog mesh			Vapor compression			Peltier effect			Adsorbent material		
	High	Moderate	Low	High	Moderate	Low	High	Moderate	Low	High	Moderate	Low
Appropriate for areas with high humidity	✓			✓			✓			✓		
Appropriate for arid areas with low humidity			✓			✓		✓		✓		
Construction cost		✓			✓			✓			✓	
Energy cost			✓	✓					✓			✓
Environmental effect			✓		✓				✓			✓
Maintenance cost			✓		✓				✓			✓
Operational cost			✓		✓			✓			✓	

1308
1309